CT- 82-100-87LR

FAA TECHNICAL CENTER
LETTER REPORT

MATH MODEL STUDY OF GLIDE SLOPE SITE FOR RUNWAY 31, LA GUARDIA AIRPORT, NEW YORK, NEW YORK

by

JOHN E. WALLS
ACT-100B.4

JULY 1982

U. S. DEPARTMENT OF TRANSPORTATION
FEDERAL AVIATION ADMINISTRATION
TECHNICAL CENTER
Atlantic City Airport, N.J. 08405

PURPOSE

The purpose of this study was to provide computer modeled Instrument Landing System (ILS) glide slope performance data for the proposed installation of a glide slope system to service runway 31 at La Guardia Airport, New York, New York.

BACKGROUND

The Eastern Region, AEA-431, plans to install a performance Category 1 ILS glide slope system to service runway 31 at La Guardia Airport, New York, New York. The terrain in the area about this runway presents several irregularities considered problematic to the formation of satisfactory glide slope signals. Instead of the flat reflecting surface which is ideal for image type glide slope signal formation, runway 31 is bounded by tidal waters at the approach end and on the right side of the runway. In addition, embankments have been constructed along these boundaries to prevent airport flooding (figure 1).

AEA-431 conducted a preliminary study and selected a proposed location for the glide glope facility which is 1,050 feet inside of runway threshold and offset 250 feet to the right of runway centerline. Because of the terrain conditions cited, a math model study of this site was requested prior to installation work. Although lateral distance/obstruction height criteria prescribes the use of a sideband reference (SBR) system for the proposed 250-foot antenna offset distance, AEA-431 requested that the modeling study include computed performance data for null reference (NR) and capture effect (CE) systems at this same location.

The request for math modeling was submitted by AEA-431 to the Airways Facility Service, Terminal Aids Branch, AAF-420, and referred to the Federal Aviation Administration (FAA) Technical Center for accomplishment.

This study was performed under Technical Program Document 07-115, Subprogram Number 071-313, Project 071-313-840, ILS Math Models. The Program Manager is Mr. Edmund A. Zyzys. Additional information regarding this study may be obtained by contacting Messrs. Jesse Jones or John Walls, at FTS-346-3807 or (609) 641-8200, extension 3807.

GENERAL

The FAA Technical Center conducted model studies through application of the Geometric Theory of Diffraction (GTD) Glide Slope Model developed by the Avionics Engineering Center, Department of Electrical Engineering, Ohio University (references 1 and 2). The GTD model was selected for this study because it considers multiple signal diffraction/reflection effects and signal shadowing by intervening terrain when computing signal energy levels arriving at the observation point (simulated aircraft position). This model was recently obtained by the Center under a multi-year task order contract with Ohio University and converted for use on the Center's Honeywell 66/60 computer. This modeling effort is the first application of the GTD glide slope model to a field site problem using the Center's computer.

While the GTD model is best suited to model the terrain affecting glide slope operation on runway 31, it does not consider the terrain located beyond the glide slope site in a direction transverse to the runway. Thus, the embankment parallel to the runway 31 is ignored by the computer program. Since effects from this embankment were of concern, it was decided to test for side embankment effects on glide slope performance using the Westinghouse Physical Optics-Plate model. This model computes object effects on glide slope performance such as a side embankment, but treats the remaining terrain as a single flat plate. Prior to GTD modeling, preliminary tests were conducted using the Westinghouse model with SBR, NR, or CE systems located at the proposed site adjacent to a single parallel embankment. The results indicated minimal effect on glide slope performance from the side embankment, and consequently the model output data are not included in this report.

The results presented in this report are considered preliminary since the ILS glide slope math models at the Technical Center have not been validated. Model validation methodology is currently being developed by Ohio University under an FAA Technical Center contract to quantitatively assess a model's performance using actual flight test data at different types of glide slope sites.

MODEL INPUT DESCRIPTION

The GTD ILS glide slope computer model requires two types of input files: (1) terrain files - which are matrices consisting of X, Y, and Z coordinate values that provide a three dimensional characterization of the terrain on the glide slope side of runway centerline from the glide slope site to beyond the middle marker, and (2) antenna/flight path files - which provide antenna data (type, heights, locations, currents, etc.) and flight path descriptors (type, start points, end points, altitude, velocity, etc.).

The terrain input files for this modeling effort were assembled from tide levels and drawings provided by AEA-431, and U.S. Geological Survey Topographical Map (7.5 Minute Series - Flushing N.Y. Quadrangle). A computer controlled digitizing system was used to collect, scale, and format these files. Figure 1 is a plan view of the approach end of runway 31 showing the proposed site location and area topography. The localizer course for runway 31 is offset 1.7°. However, the terrain files and the glide slope approach path were modeled for a centerline approach. This factor is considered to have minimal effect on the results obtained since terrain differences for this angular offset are very small.

The computer model applies an interpolation process to the terrain files to determine a new terrain profile for each observation point (simulated aircraft position) along the flight path. The new profile is that of the terrain directly below a line drawn from the ILS antenna to the observation point. This profile is the reflecting surface used in the GTD computation of the glide slope energy at the observation point. Figure 2 is a composite of terrain profiles computed at 1,000-foot intervals along the approach path for the low tide condition.

Figures 3 and 4 are composites of terrain profiles similarly computed for the mean and high tide conditions, respectively. These profiles are representative of the terrain modeled. The actual profile interval utilized in the model computations was 170 feet.

Antenna heights for the proposed site simulations were computed to produce actual path angles of approximately 3°. Antenna current phasing for all simulations were computed using a simulation of the airborne reference phasing techniques detailed in the Flight Inspection Manual OAP 8200.1 (reference 3). In the simulation, samples of antenna current phase are recorded while flying the simulated aircraft along an approach angle of 1.5° from 8 to 4 nautical miles, with respect to the site. Ten samples of antenna current phase are recorded for each antenna. Using average phase values, the phase of the upper antenna is adjusted for zero phase difference with respect to the phase of the lower antenna for sideband reference or null reference systems. For capture effect systems, the phases of the lower and upper antennas are adjusted to result in zero phase differences with respect to the middle antenna. This technique is similar to the method originated by the Ohio University Avionics Center for their math modeling applications. Antenna current phasing runs performed for each of the three tide conditions resulted in slightly different phase values. These results were averaged to obtain the phase values which were used for all subsequent modeling runs regardless of tidal state. The antenna heights, antenna current-amplitude/phase, and A-ratio values used in this study are listed in table 1. An altitude of 1,250 feet, with respect to the site, was used for all level run simulations.

DATA PRESENTATION

Math modeling results are provided on 18 data plots which are divided by figure number into 3 groups of 6 plots each according to the glide slope system modeled. Figure numbers 5, 6, and 7 identify SBR, NR, and CE computed performance plot results, respectively. Each figure number is followed by letter designators A through F which identify specific plots within the group. The 6 plots within the group are further divided into 3 pairs of plots. A plot pair provides system performance results for each of the 3 tide levels modeled: low, mean, and high tide.

Each plot pair consists of a glide path structure plot and a level run plot. The path structure plot shows modeled glide path structure (microamps) versus distance from runway threshold (feet). This plot is directly comparable with the first error trace as recorded by FAA Automatic Flight Inspection (AFIS) aircraft. The second plot of the pair is a level run plot showing course deviation indication (CDI) current in microamps versus approach elevation angle in degrees.

The scheme for letter designators is as follows: Letters A and B designate the structure and level run plots for low tide condition; C and D indicate the structure and level run plots for mean tide; E and F indicate the structure and level run plots for high tide conditions. With this scheme, one can compare the structure runs for each of the three antenna systems at low tide by selecting figures 5A, 6A, and 7A. Level run, low tide comparisons can be made by selecting the B lettered plots of figures 5, 6, and 7 for comparison, and so forth.

Table 2 summarizes actual path angle, path width, and symmetry (± 75 microamp CDI current) data as presented on individual plots (figures 5A through 7F).

DATA ANALYSIS

Table 2 provides a convenient reference for assessing the effect of tide level on glide slope performance parameters. The computed glide slope performance parameters for the CE system remain fairly constant with change in tide while the NR system is most affected by tidal variation. The glide path width of the NR system decreases 0.12° between high and low tide levels. The direction of change and non-linear relationship of path width variation with tide level should be considered during system installation and system performance assessment.

Examination of plotted results (figures 5A through 7F) reveals that poorest performance for all three systems should be obtained during low tide conditions. However, even at low tide acceptable path structure performance is indicated for all three systems in Zone 2 (24,300 to 3,500 feet from threshold). All path structure results show large excursions of fly down CDI error in Zone 3 (3,500 feet to runway threshold). This excursion in CDI is characteristically obtained with upsloped terrain such as the embankment at the approach end of the runway (reference 1).

Examination of plotted level runs results indicate a possible problem with satisfactory clearance signals at low approach angles with the SBR and CE systems during low tide (figures 5B and 7B). The remaining level run plots for the SBR and CE systems indicate acceptable course width and linearity performance.

CONCLUSIONS

Modeled results indicate satisfactory path structure performance should be obtained in Zone 2 withthe SBR, NR, and CE systems installed at the proposed location. Computed CE system path structure is superior, but the higher antennas heights needed by this system exceed allowable obstruction height/distance from runway criteria. For this reason, the SBR system is considered the best choice of the available image type glide slope systems for this installation.

Two potential system performance problems are indicated in the modeled results: (1) large fly down CDI errors in Zone 3, (2) clearance signal level may be marginal at low approach angles during low tide.

TABLE 1. ANTENNA INPUT DATA
RUNWAY 31 LA GUARDIA, NEW YORK

ANTENNA SYSTEM	ANTENNA HEIGHTS (FEET)	A RATIO (1)	ANTENNA CURRENT - AMPLITUDE/PHASE		
			ISS (2)	ICS (3)	ICC (4)
SBR	Lower 7.30	0.351	-1.0/0.0°	1.0/0.0°	0.0/0.0°
	Upper 21.28		1.0/-3.9°	-.0/0.0°	0.0/0.0°
NR	Lower 14.80	0.342	0.0/0.0°	1.0/0.0°	0.0/0.0°
	Upper 29.60		1.0/-0.2°	0.0/0.0°	0.0/0.0°
CE	Lower 14.27	0.351	-0.5/0.3°	1.0/0.3°	0.484/0.3°
	Middle 28.54		1.0/0.0°	-0.5/0.0°	0.0/0.0°
	Upper 42.81		-0.5/2.1°	0.0/0.0°	0.484/2.1°

(1) A Ratio - Ratio of separate sideband amplitude to carrier sideband signal amplitude.

(2) ISS - Separate sideband current.

(3) ICS - Carrier sideband current.

(4) ICC - Clearance carrier current.

TABLE 2. SUMMARY - GLIDE PATH DATA

RUNWAY 31 LA GUARDIA, NEW YORK

ANTENNA SYSTEM	TIDE	ACTUAL ANGLE (DEGREES)	WIDTH (DEGREES)	SYMMETRY (% 90 Hz/150Hz)
SBR	Low	3.05	0.73	59/41
	Mean	3.01	0.71	57/43
	High	2.98	0.65	55/45
NR	Low	3.06	0.79	60/40
	Mean	3.01	0.76	58/42
	High	2.97	0.67	55/45
CE	Low	3.01	0.74	53/47
	Mean	3.00	0.69	50/50
	High	3.00	0.65	50/50

References:

1. In Service Improvements and Modernization of All Components of the Instrument Landing Systems, DOT/FAA/ Report No. FAA-RD-78-112, Vol. 1, 1978.

2. GTD Terrain Reflection Model Applied to ILS Glide Slope IEEE Transactions on Aerospace and Electronic Systems, Vol. AES-18, No. 1, January 1982.

3. United States Flight Inspection Manual, FAA Handbook OAP 8200.1, Change 32, Section 217.

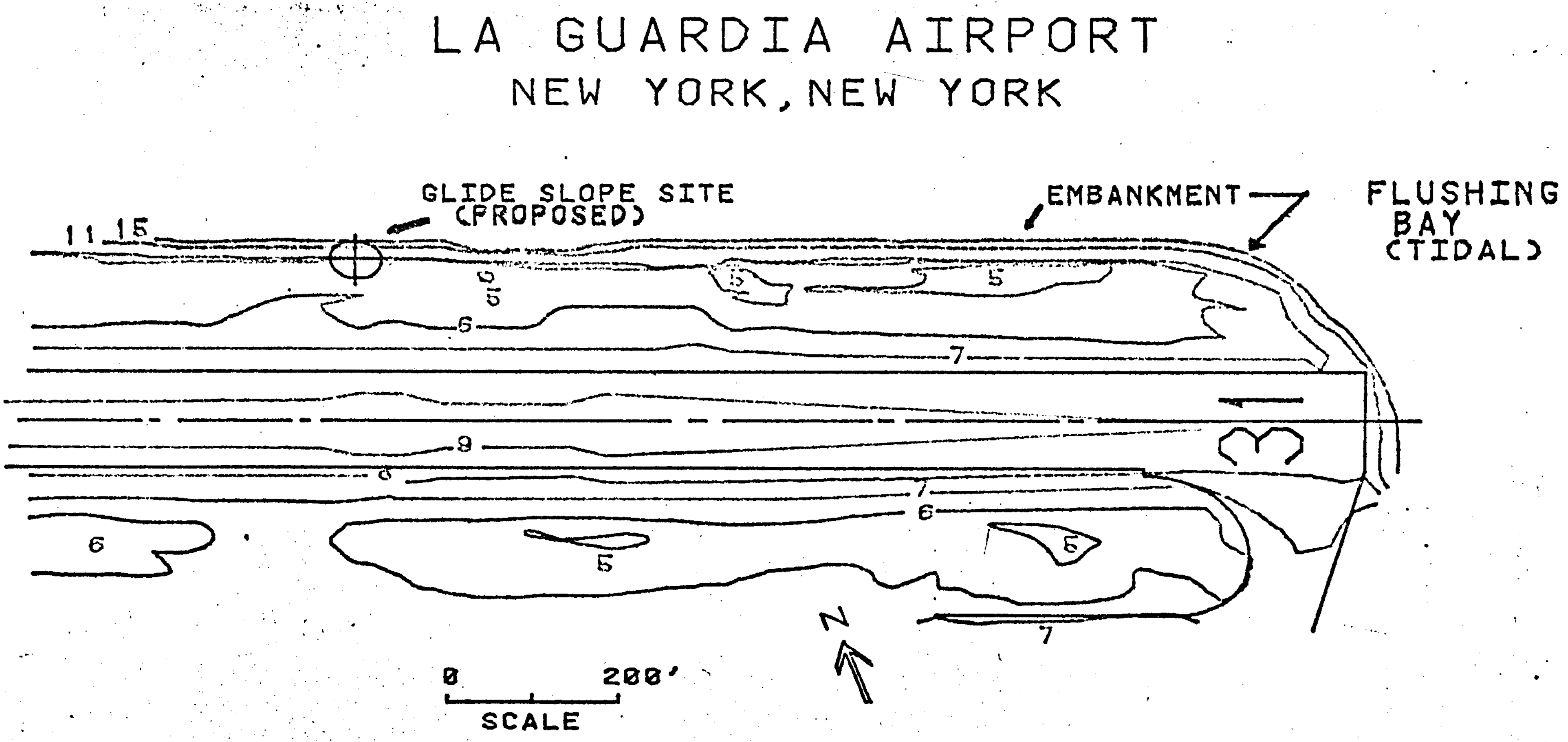

FIGURE 1 - RUNWAY 31, PROPOSED SITE AND TOPOGRAPHY

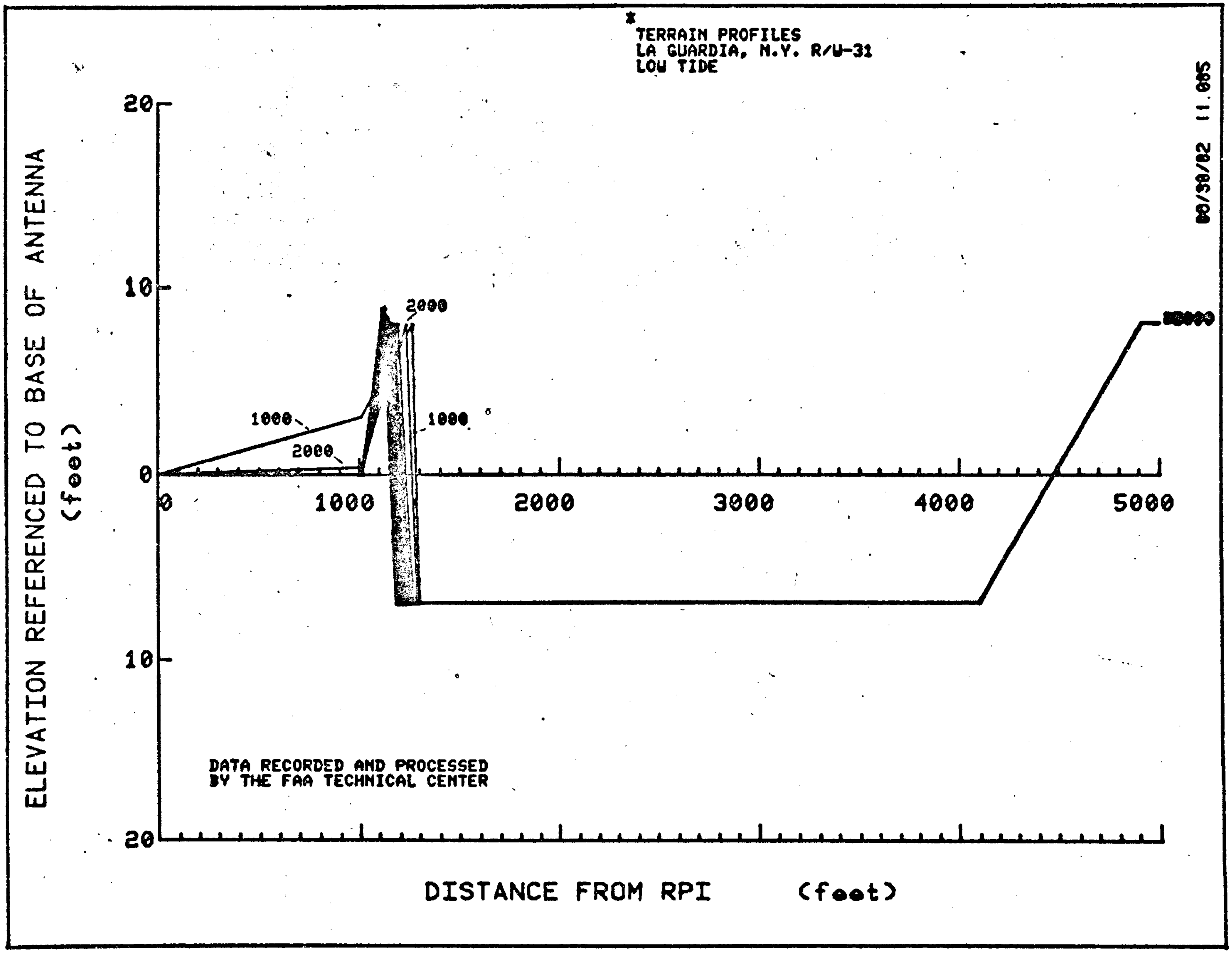

FIGURE 2 - COMPOSITE OF TERRAIN PROFILES, LOW TIDE

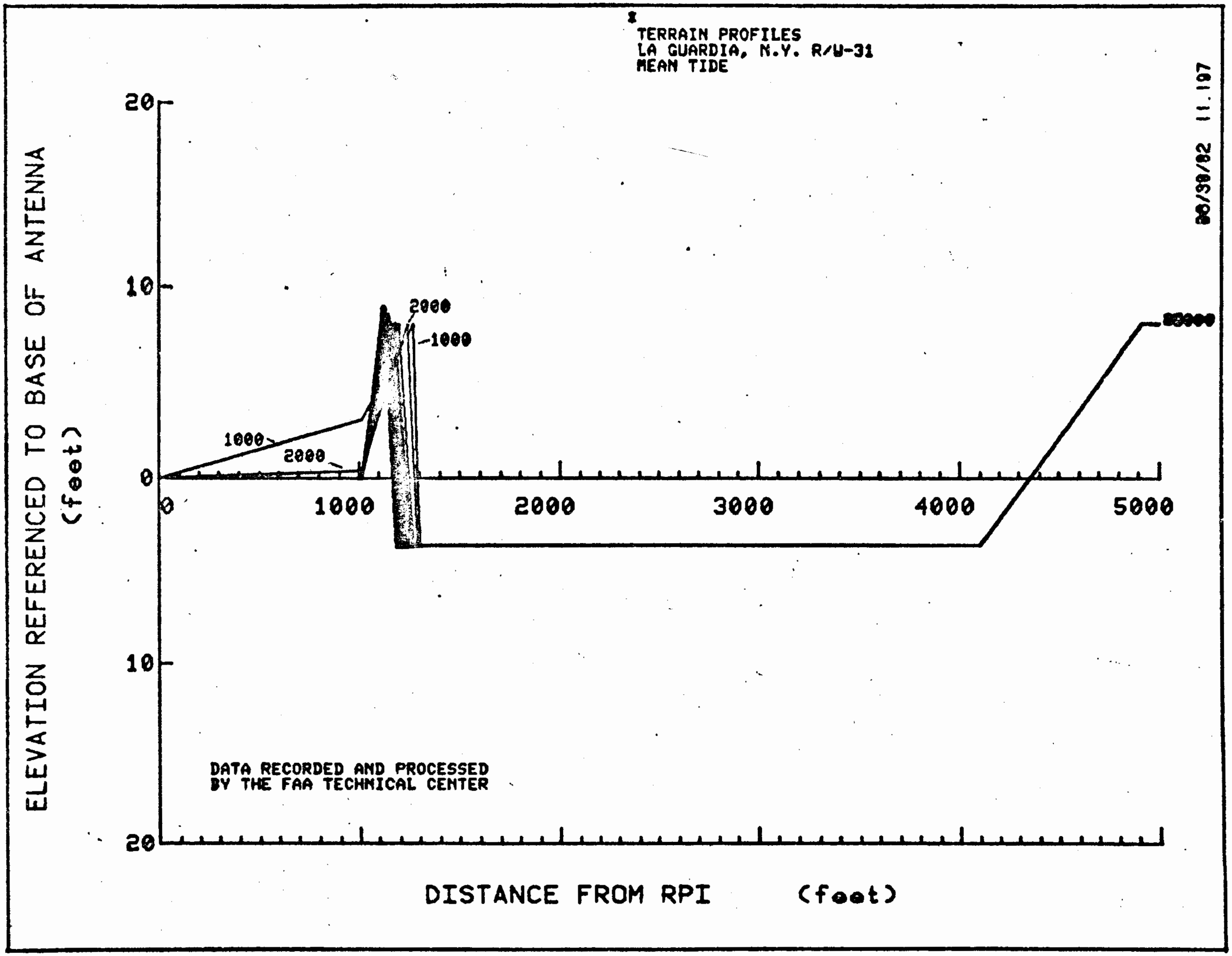

FIGURE 3 - COMPOSITE OF TERRAIN PROFILES, MEAN TIDE

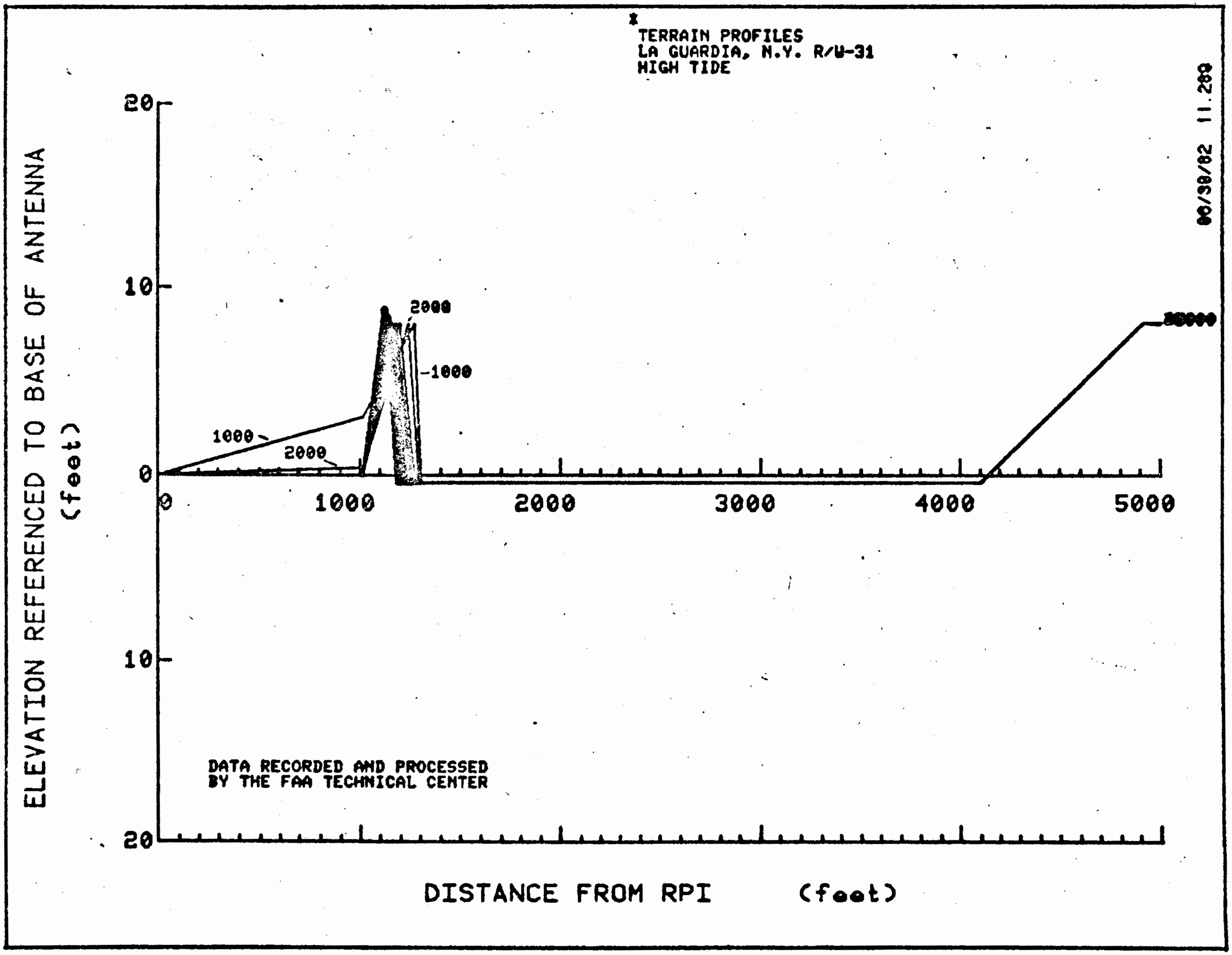

FIGURE 4 - COMPOSITE OF TERRAIN PROFILES, HIGH TIDE

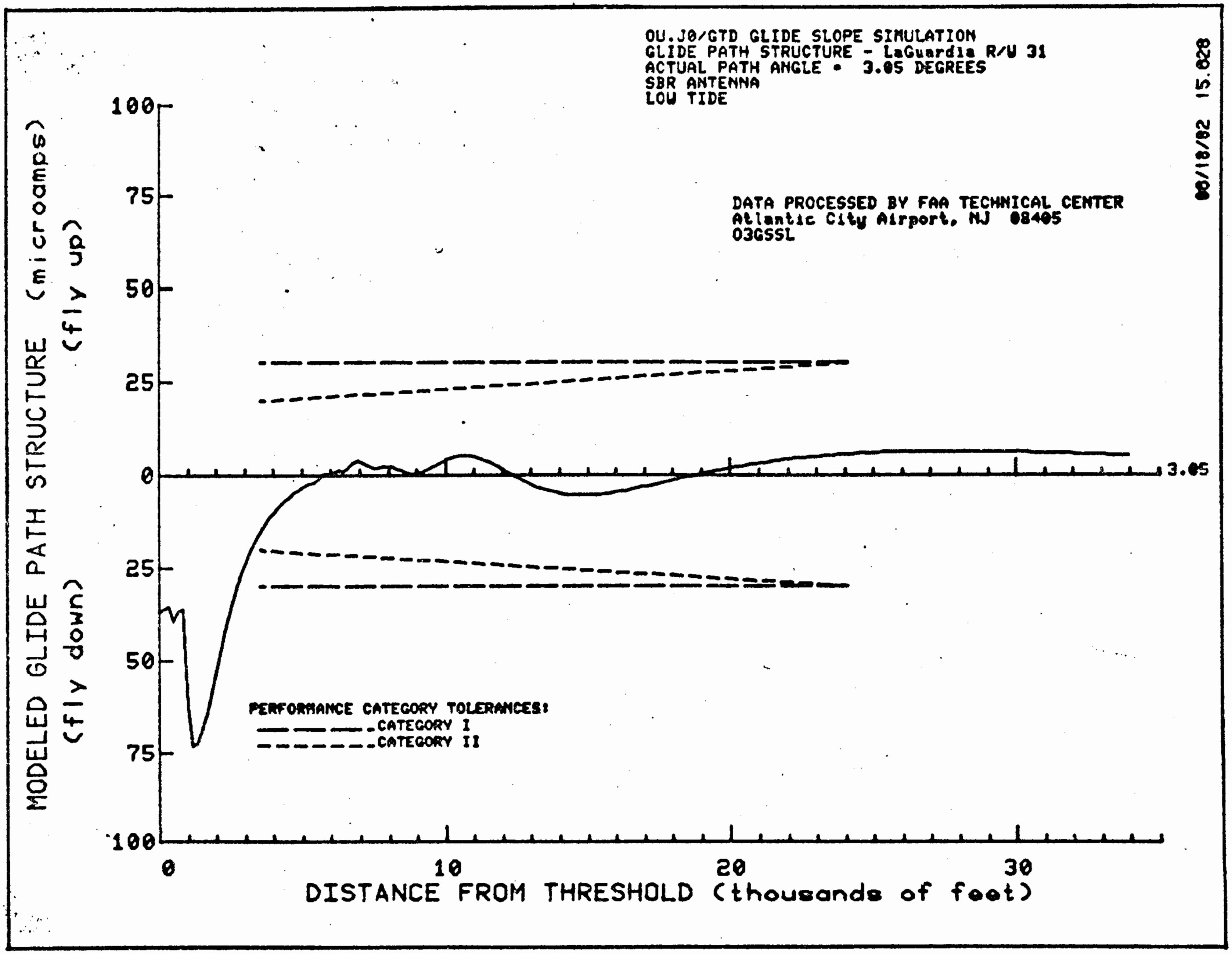

FIGURE 5A - MODELED PATH STRUCTURE, SBR SYSTEM, LOW TIDE

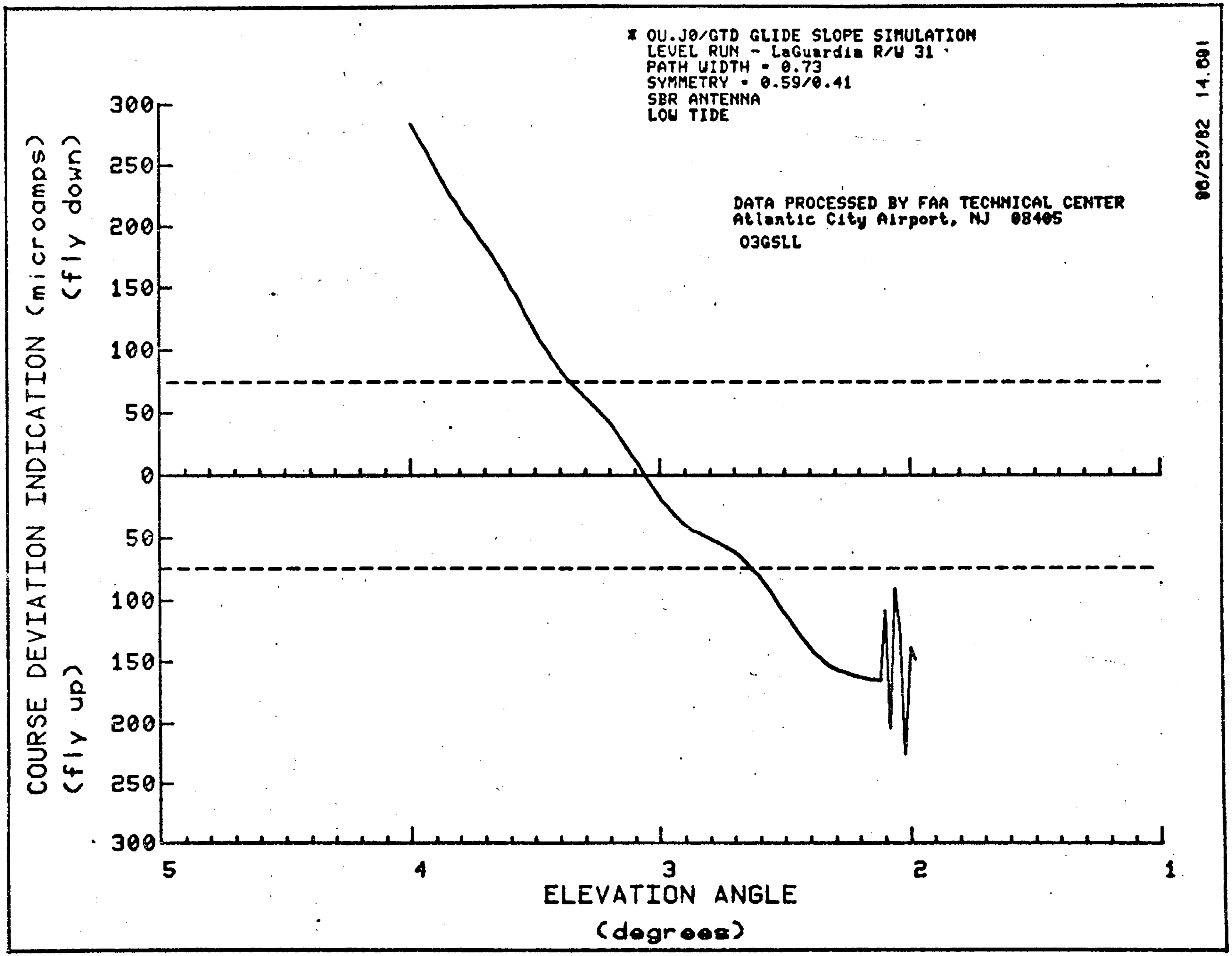

FIGURE 5B - MODELED LEVEL RUN, SBR SYSTEM, LOW TIDE

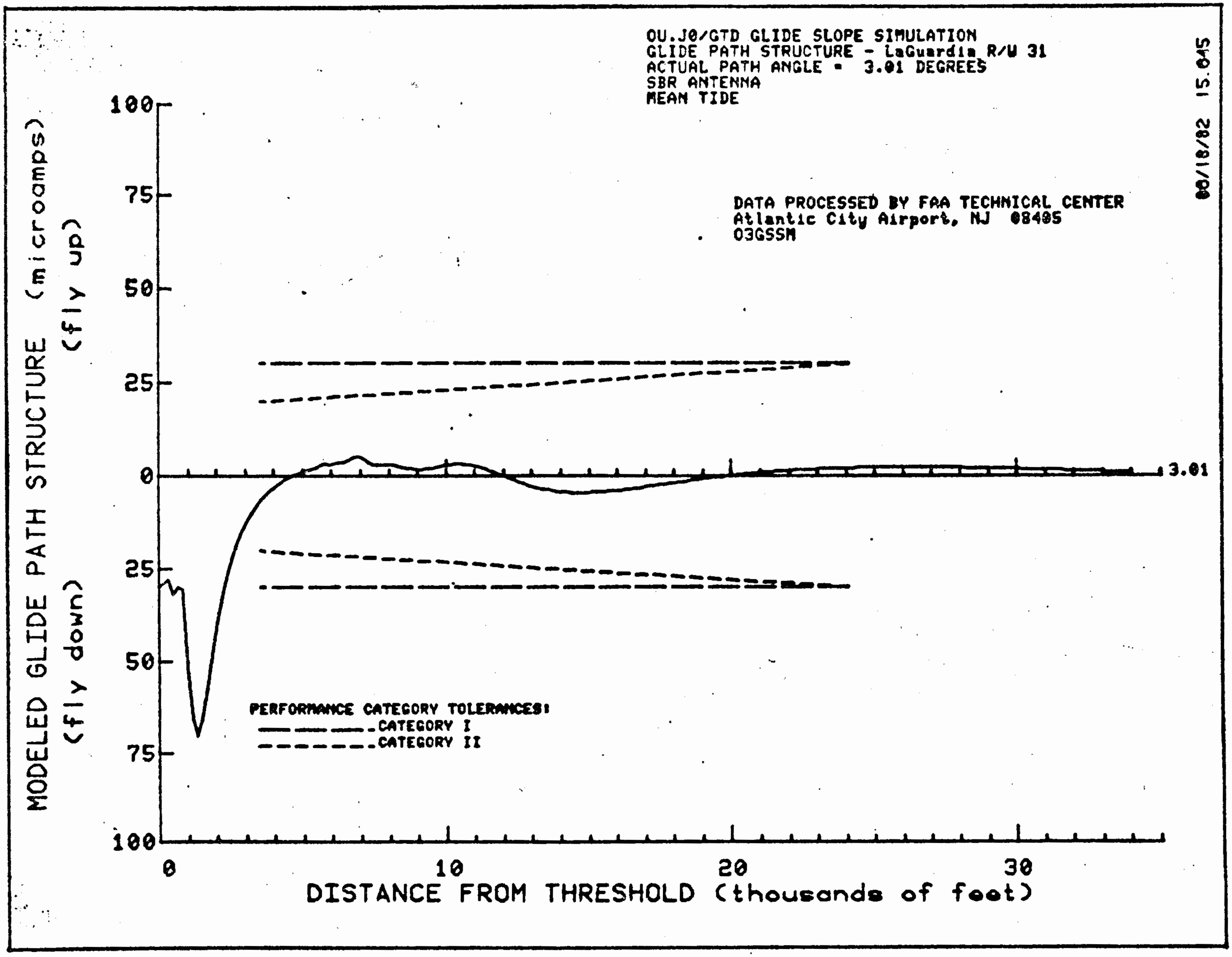

FIGURE 5C - MODELED PATH STRUCTURE, SBR SYSTEM, MEAN TIDE

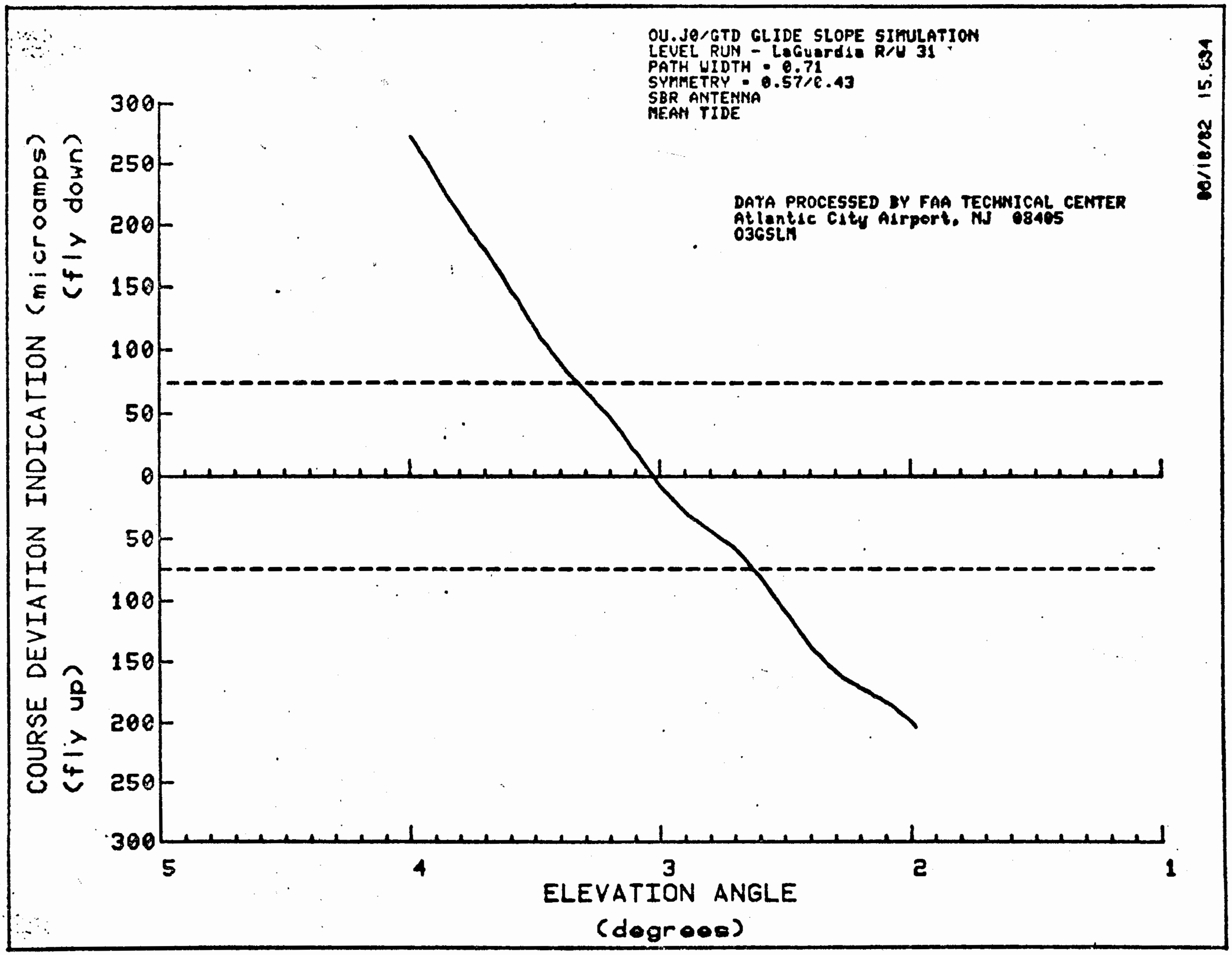

FIGURE 5D - MODELED LEVEL RUN, SBR SYSTEM, MEAN TIDE

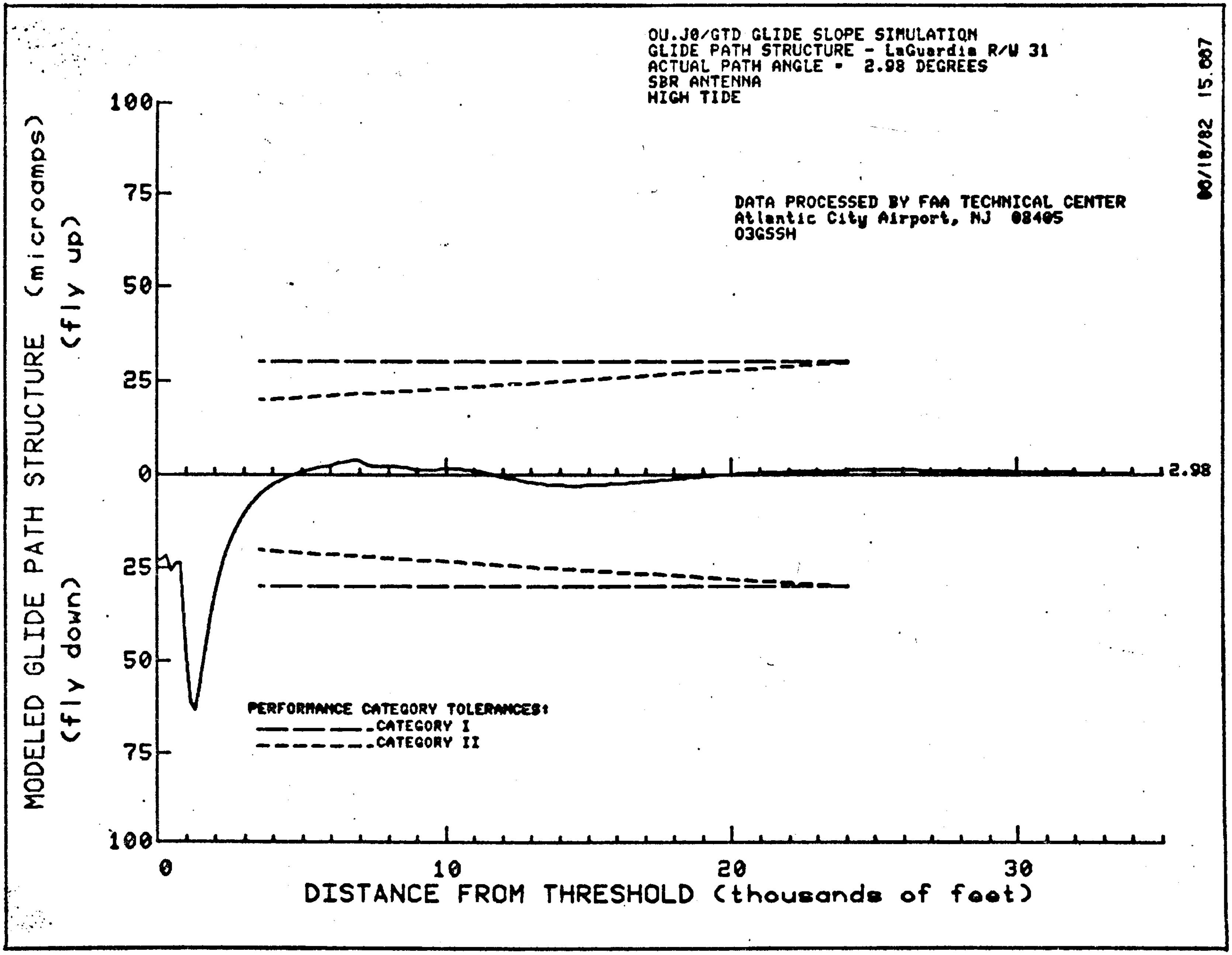

FIGURE 5E - MODELED PATH STRUCTURE, SBR SYSTEM, HIGH TIDE

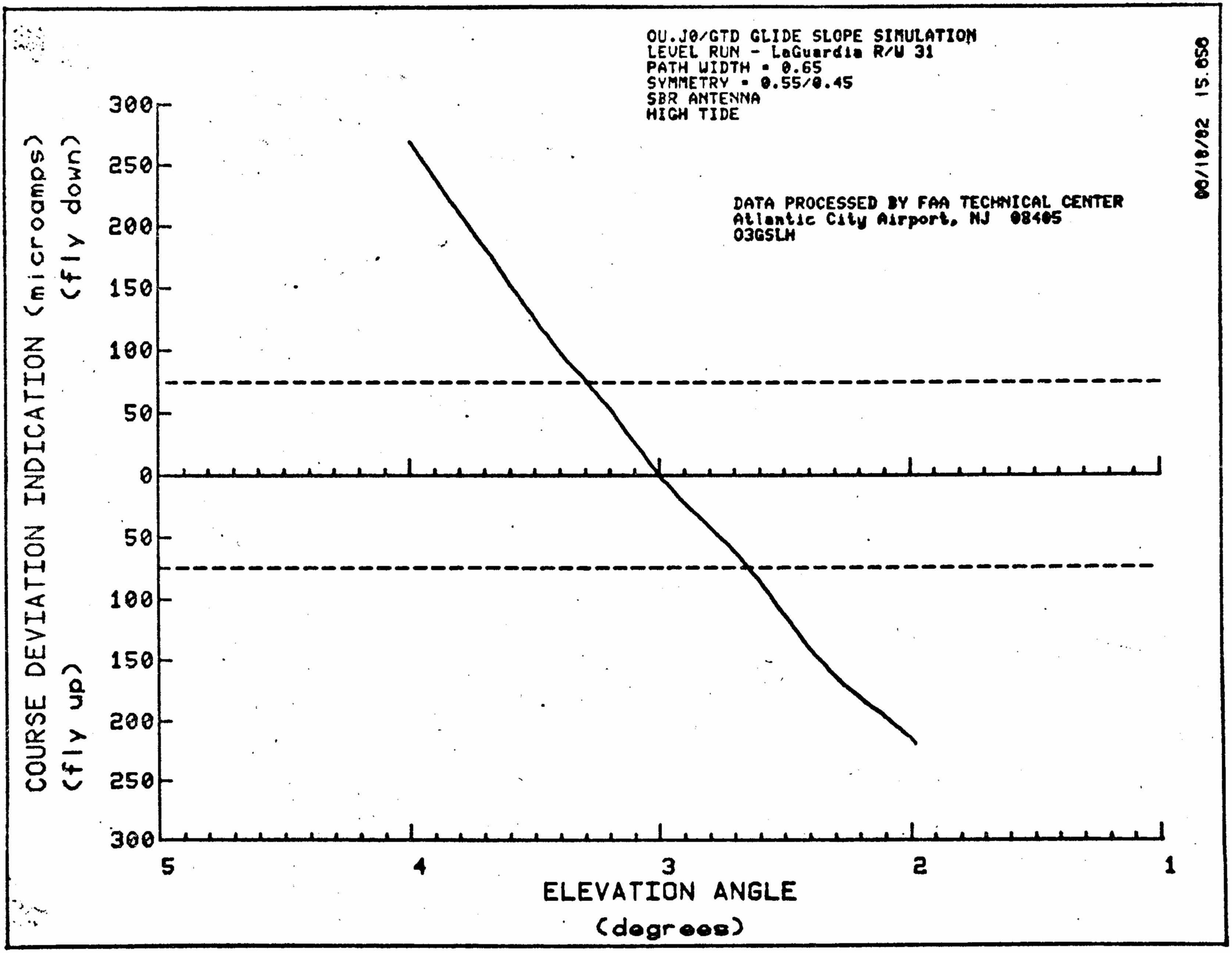

FIGURE 5F - MODELED LEVEL RUN, SBR SYSTEM, HIGH TIDE

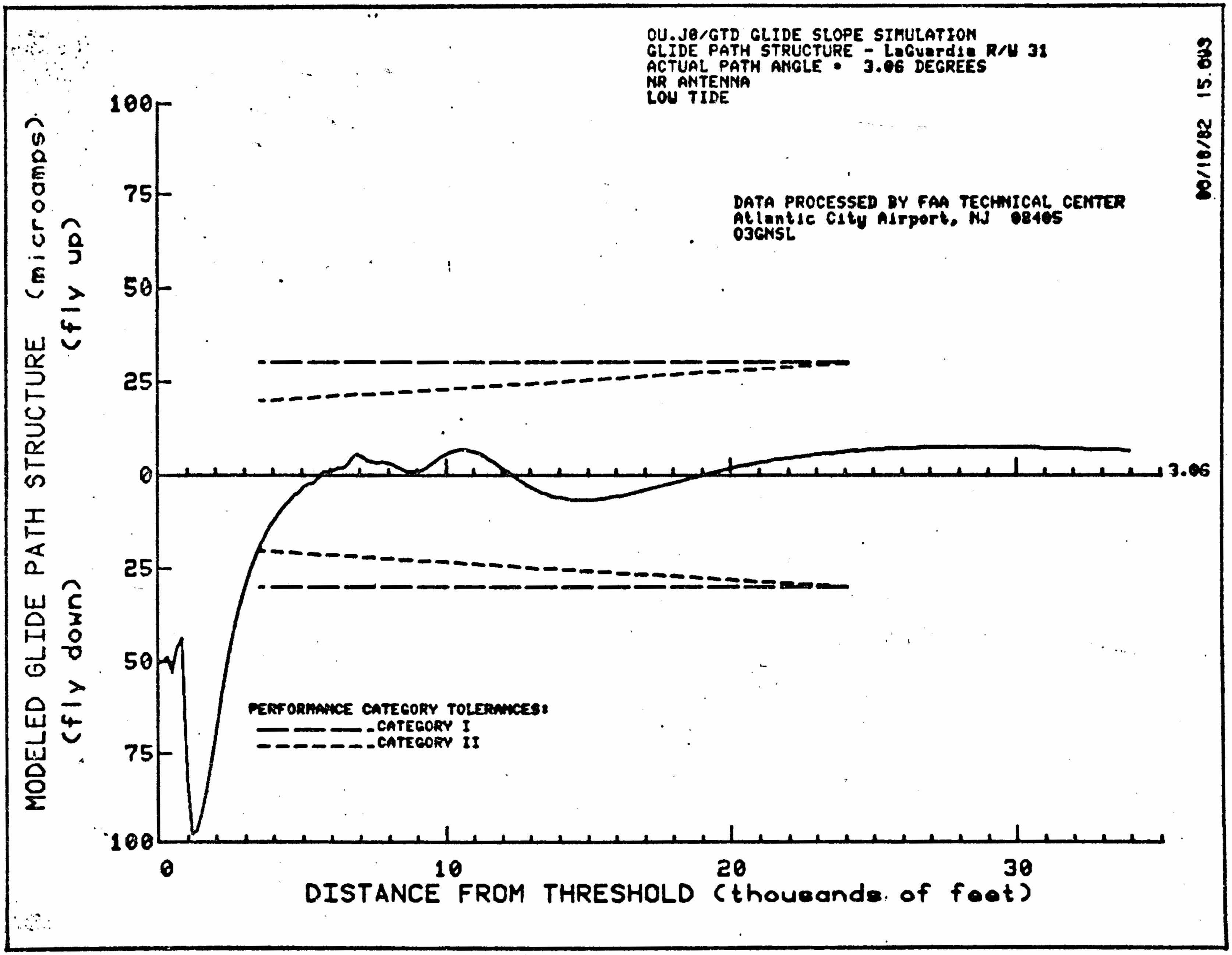

FIGURE 6A - MODELED PATH STRUCTURE, NR SYSTEM, LOW TIDE

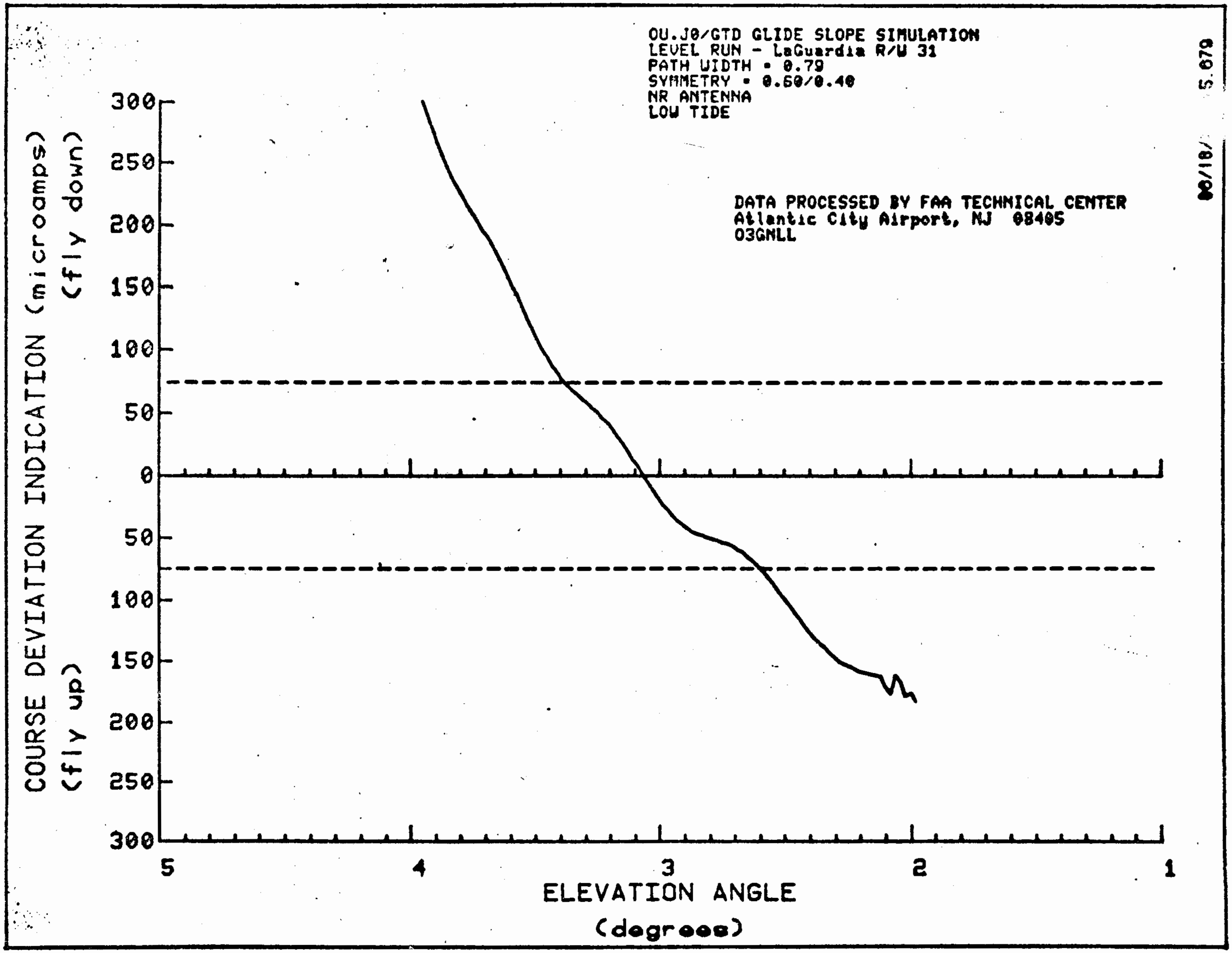

FIGURE 6B - MODELED LEVEL RUN, NR SYSTEM, LOW TIDE

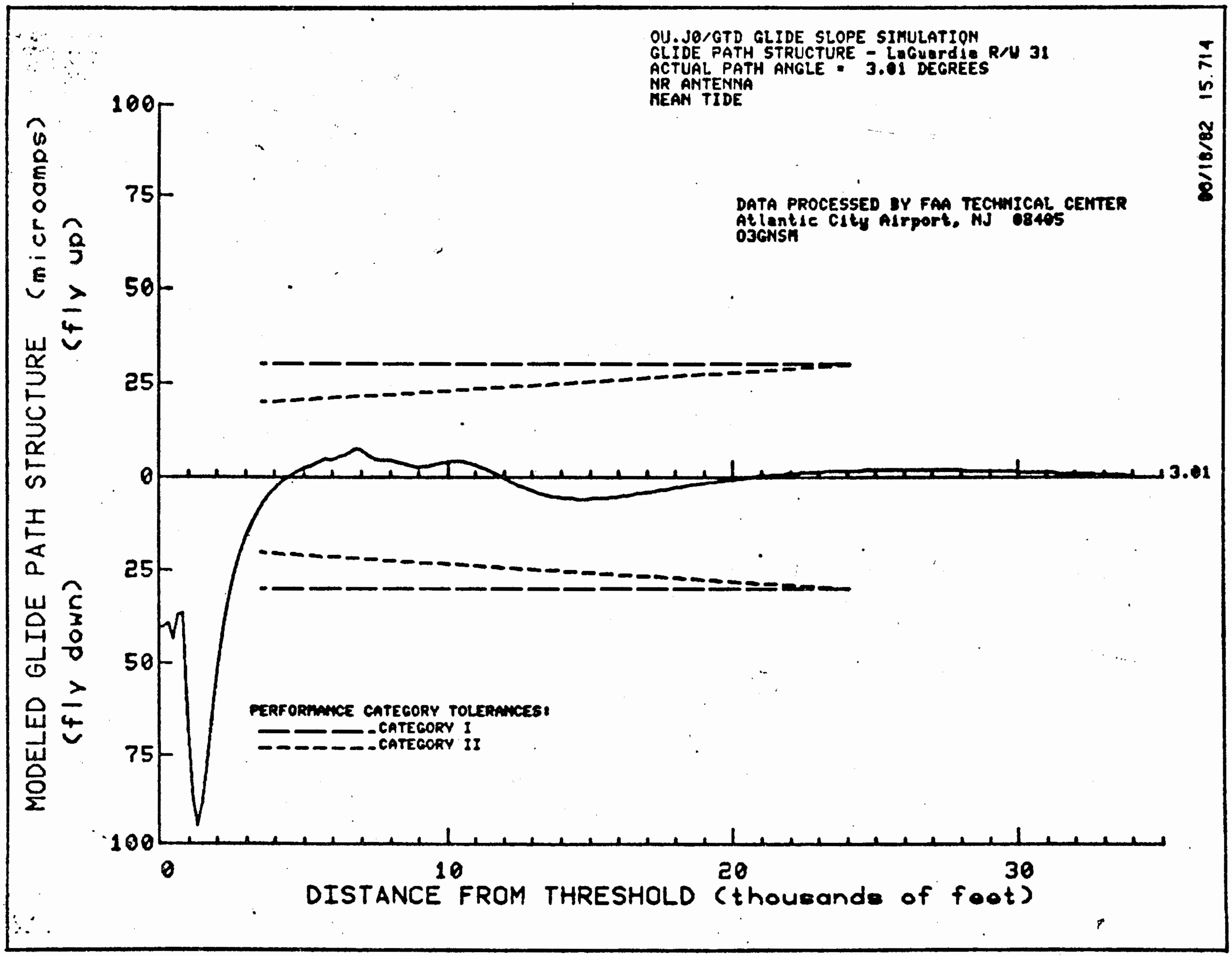

FIGURE 6C - MODELED PATH STRUCTURE, NR SYSTEM, MEAN TIDE

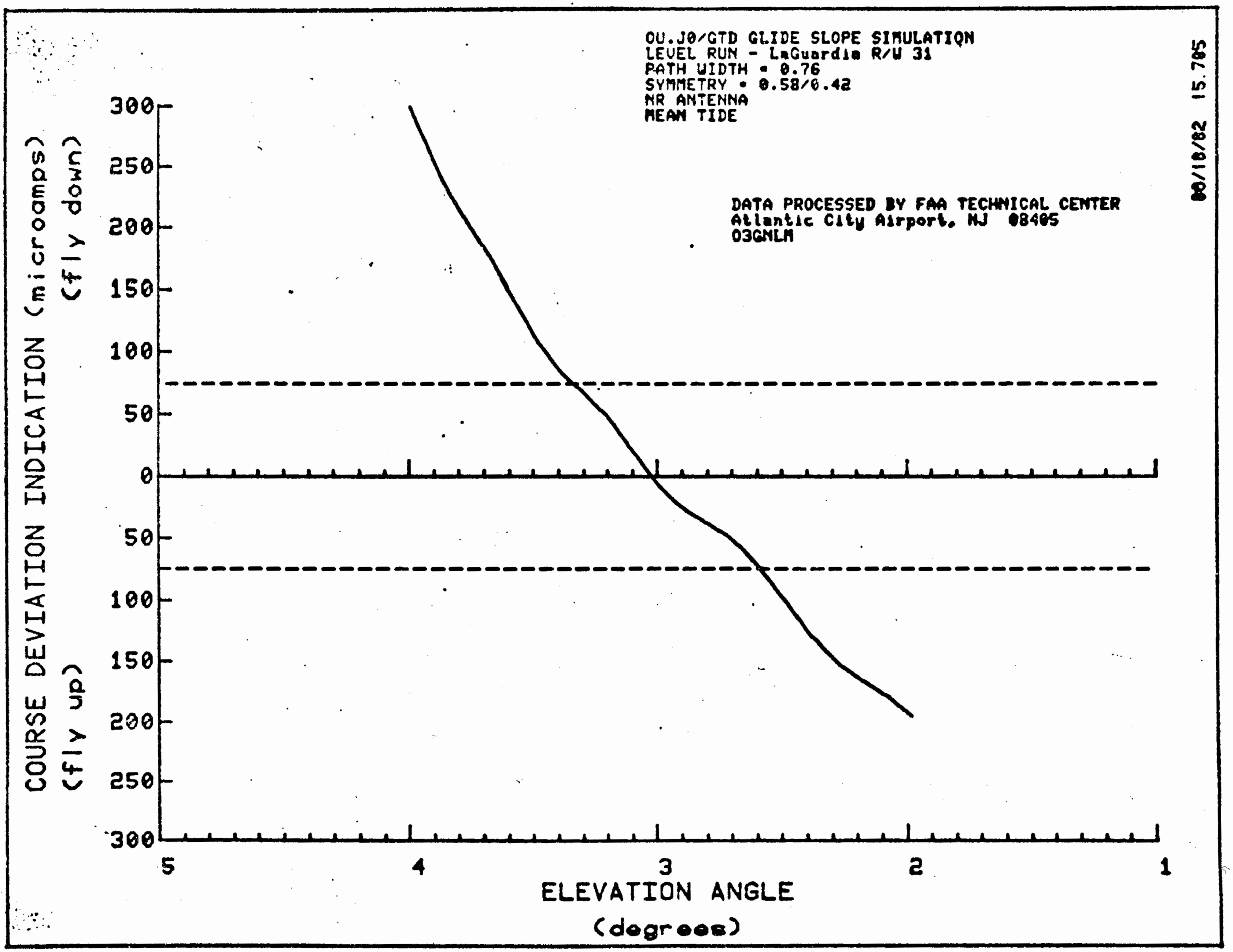

FIGURE 6D - MODELED LEVEL RUN, NR SYSTEM, MEAN TIDE

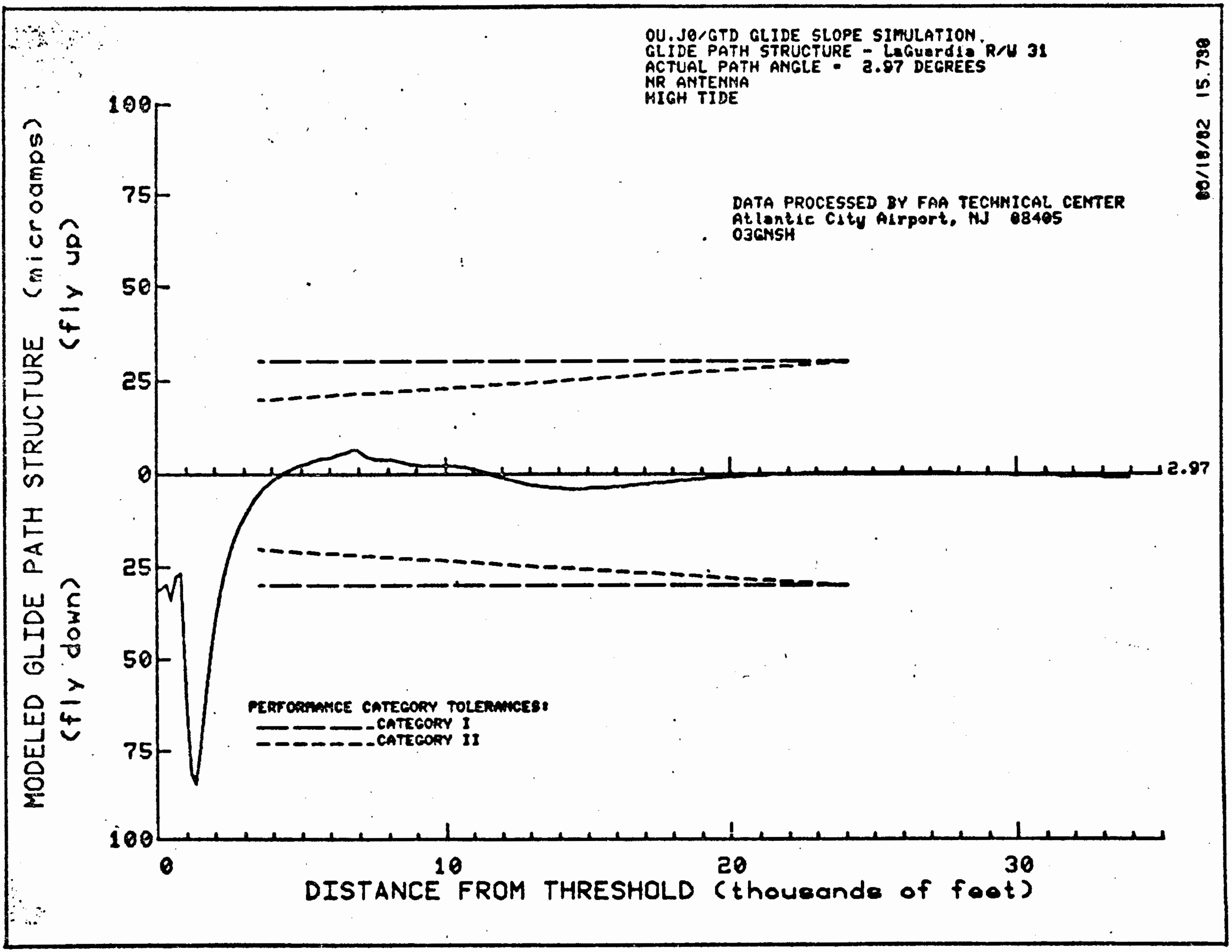

FIGURE 6E - MODELED PATH STRUCTURE, NR SYSTEM, HIGH TIDE

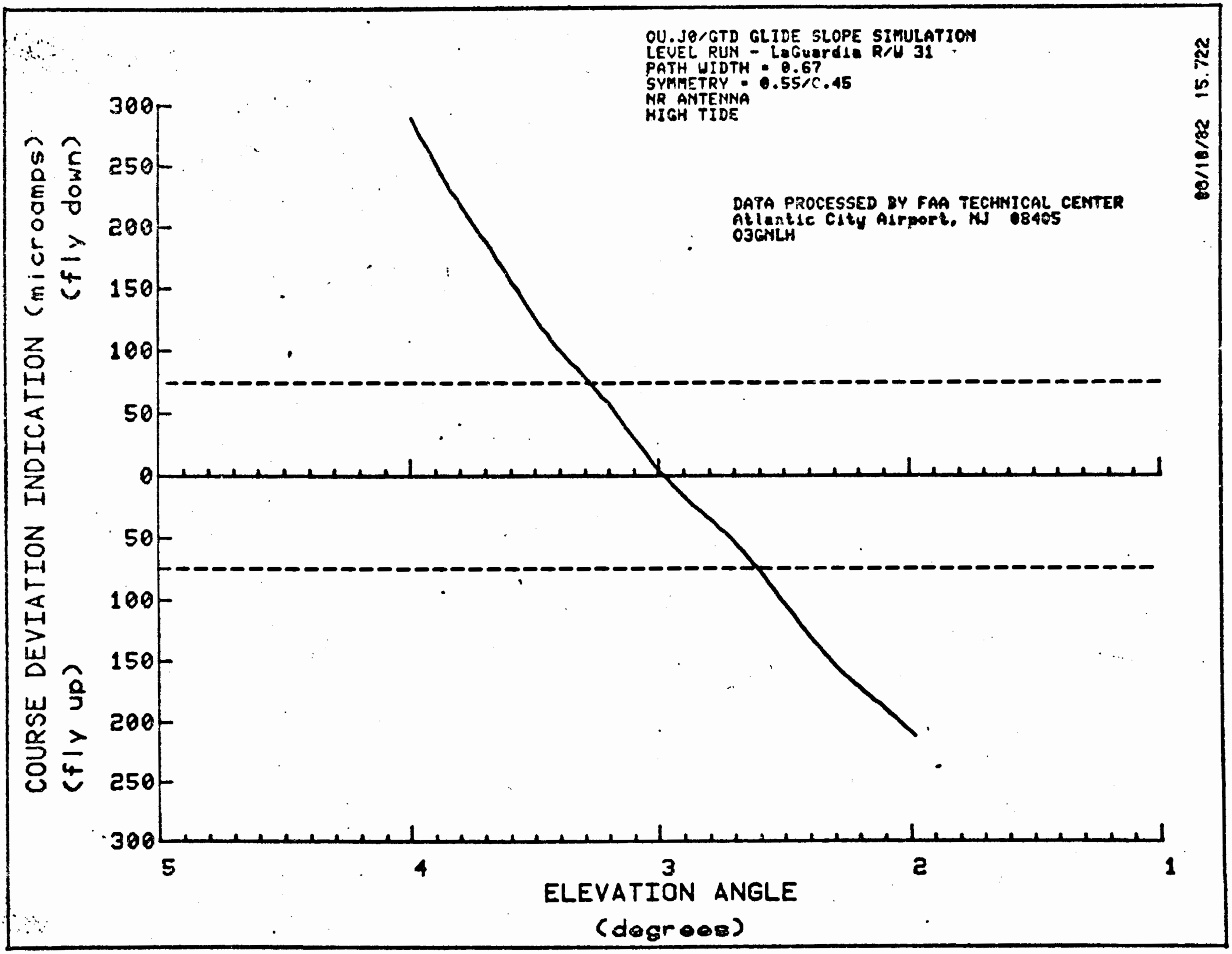

FIGURE 6F - MODELED LEVEL RUN, NR SYSTEM, HIGH TIDE

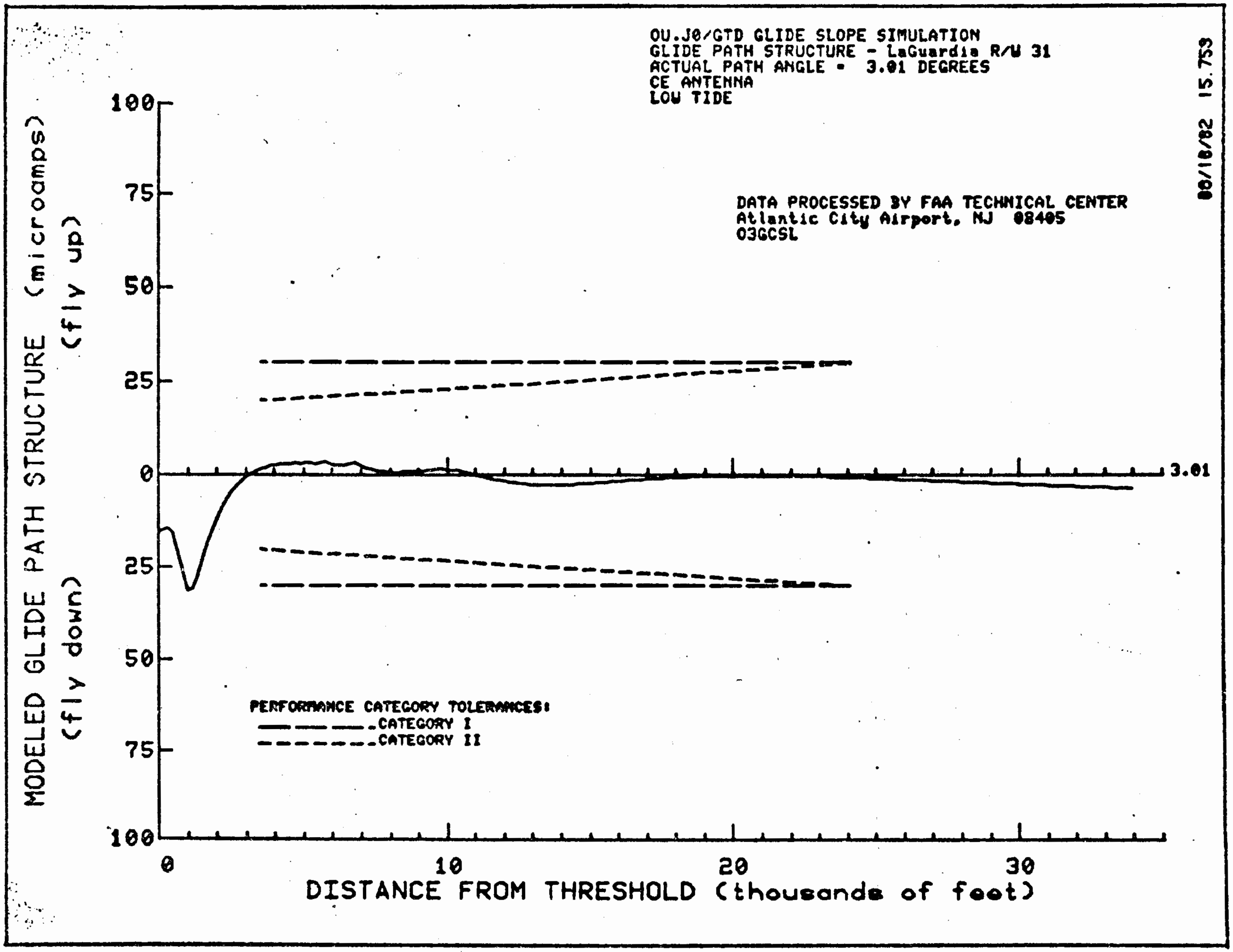

FIGURE 7A - MODELED PATH STRUCTURE, CE SYSTEM, LOW TIDE

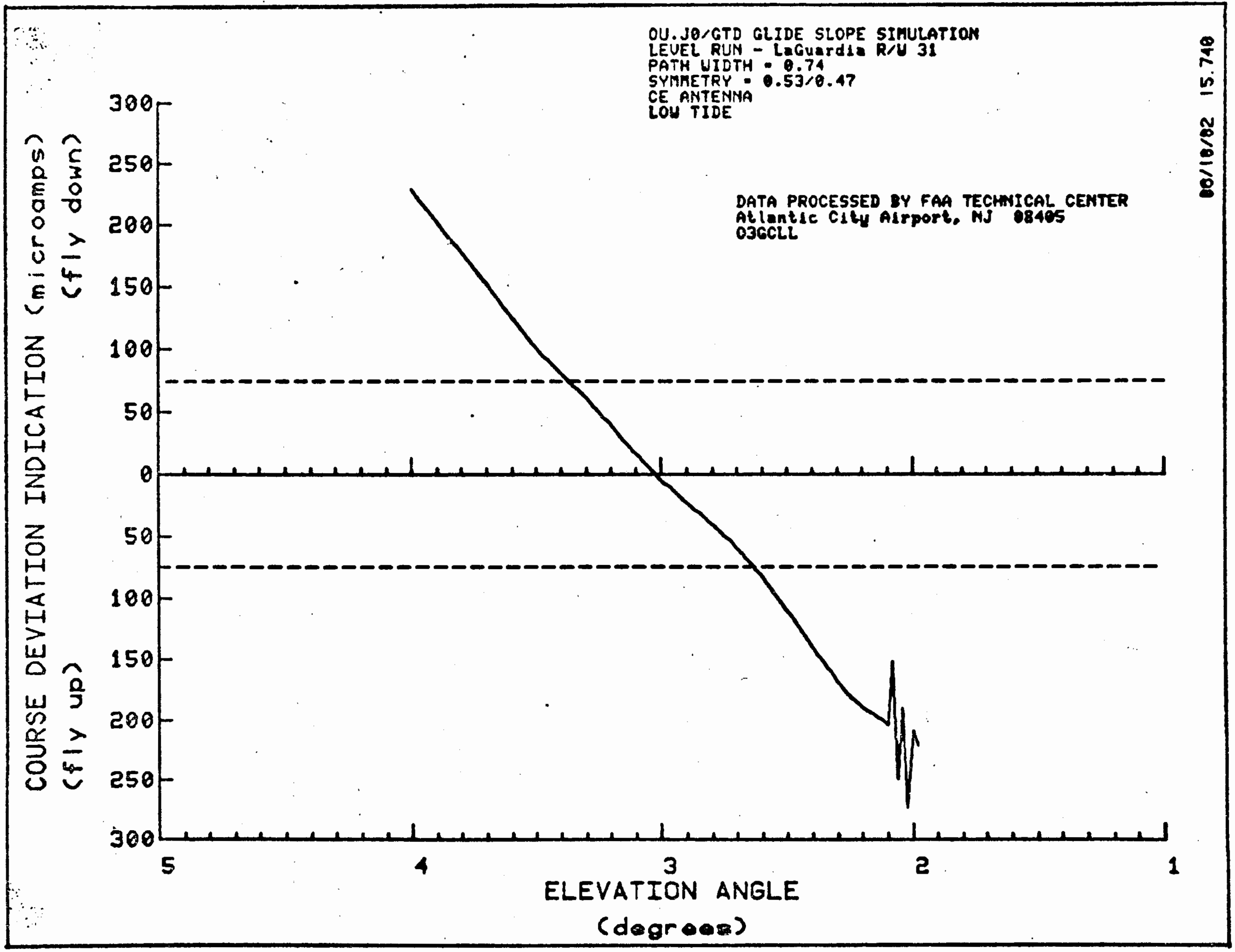

FIGURE 7B - MODELED LEVEL RUN, CE SYSTEM, LOW TIDE

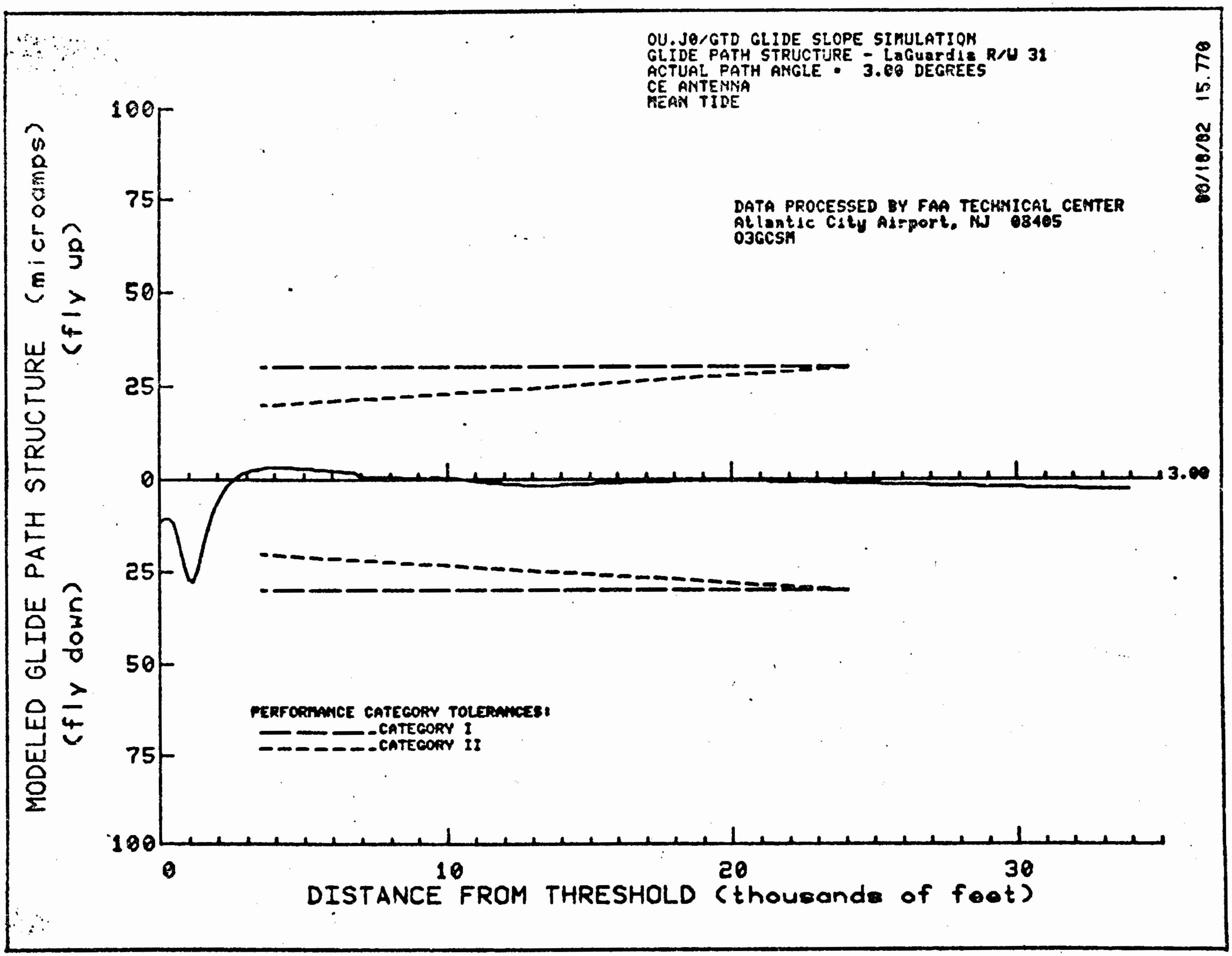

FIGURE 7C - MODELED PATH STRUCTURE, CE SYSTEM, MEAN TIDE

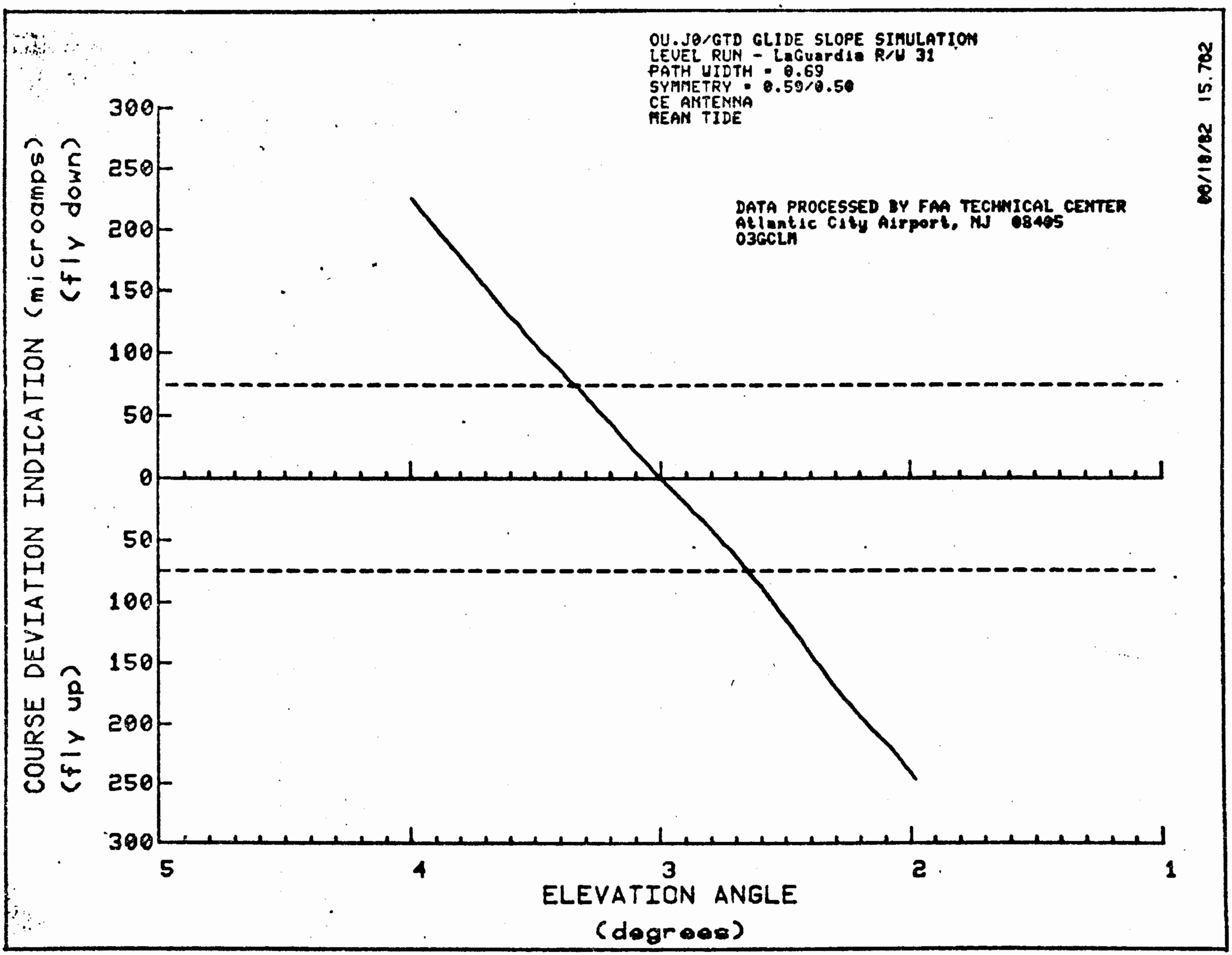

FIGURE 7D - MODELED LEVEL RUN, CE SYSTEM, MEAN TIDE

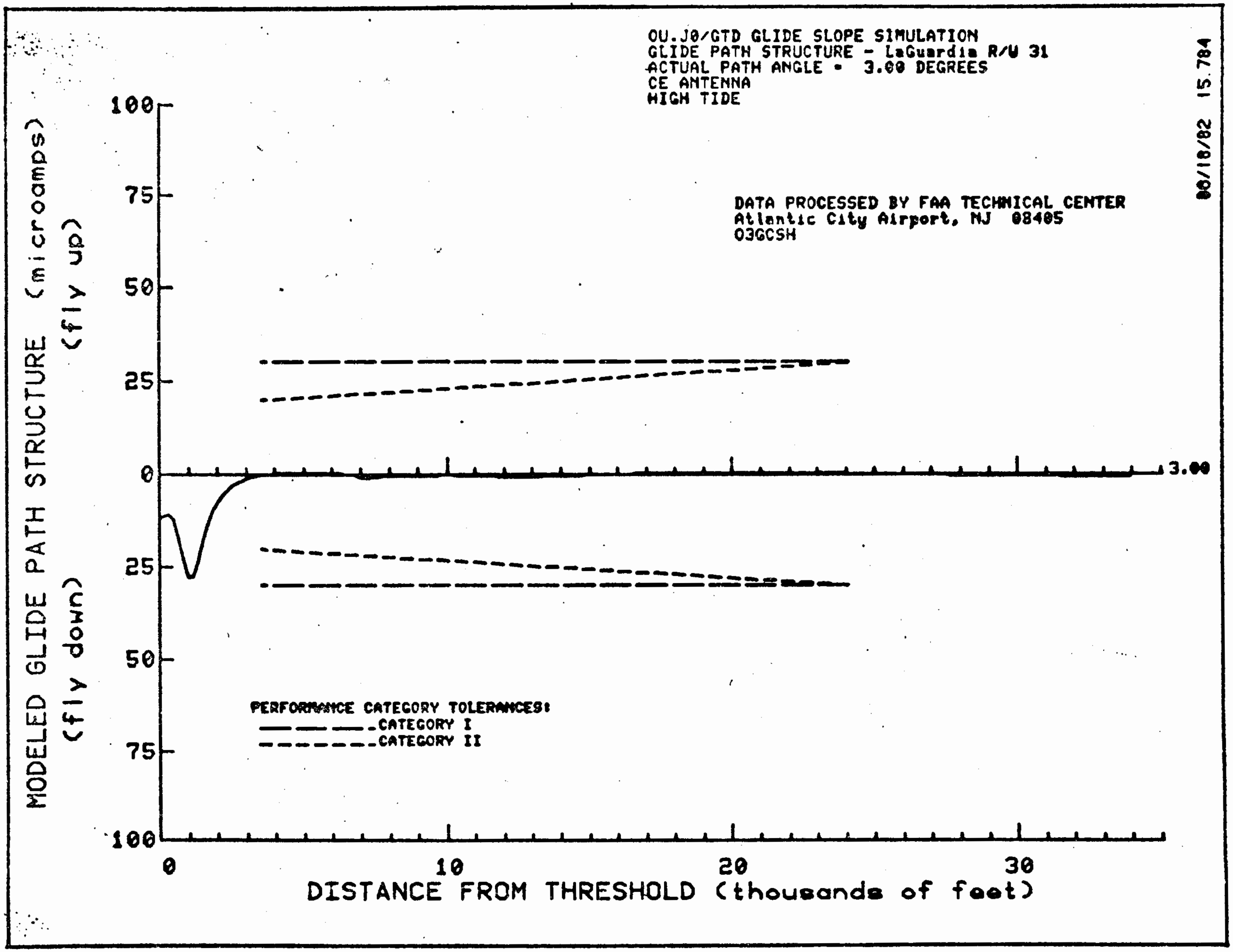

FIGURE 7E - MODELED PATH STRUCTURE, CE SYSTEM, HIGH TIDE

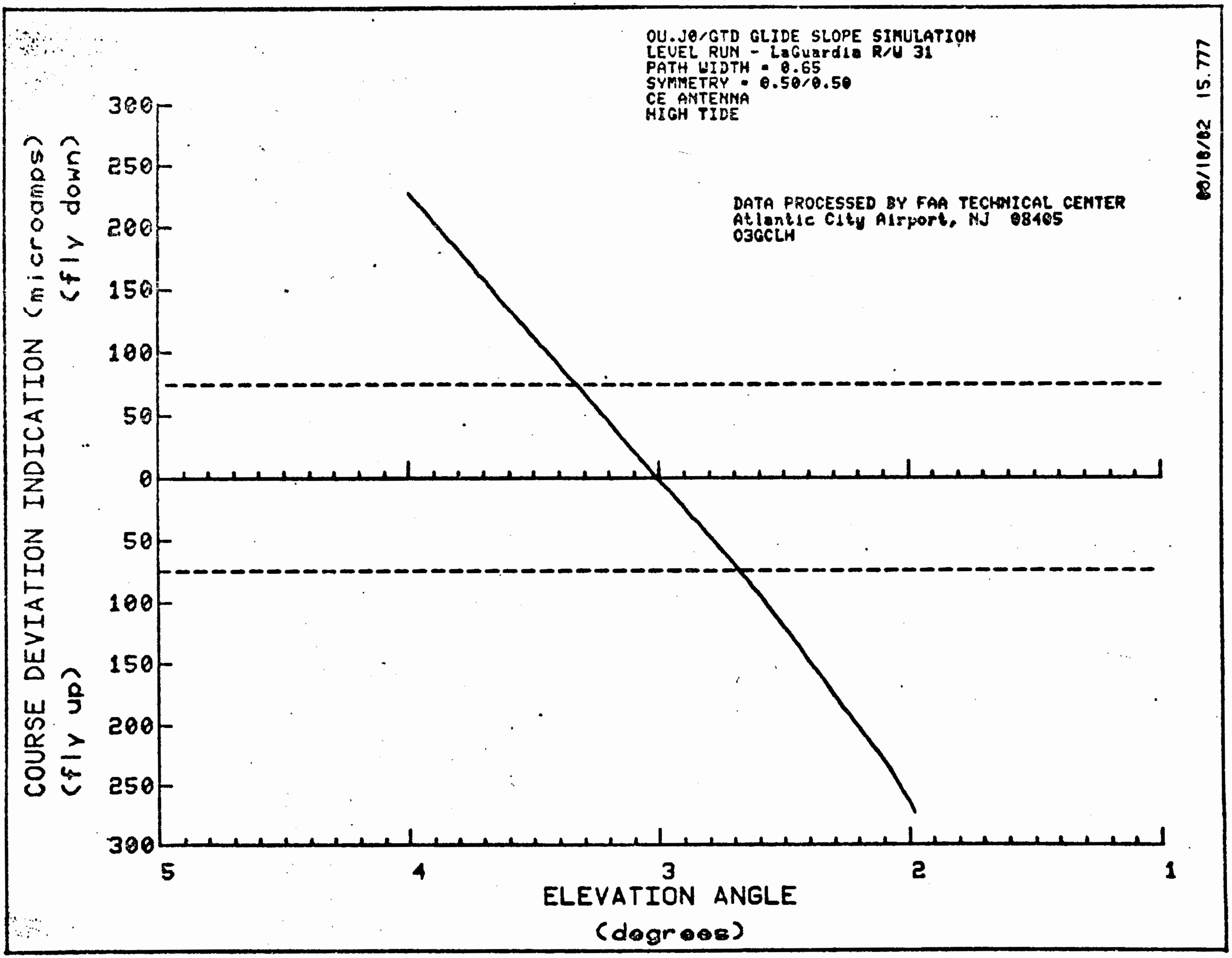

FIGURE 7F - MODELED LEVEL RUN, CE SYSTEM, HIGH TIDE

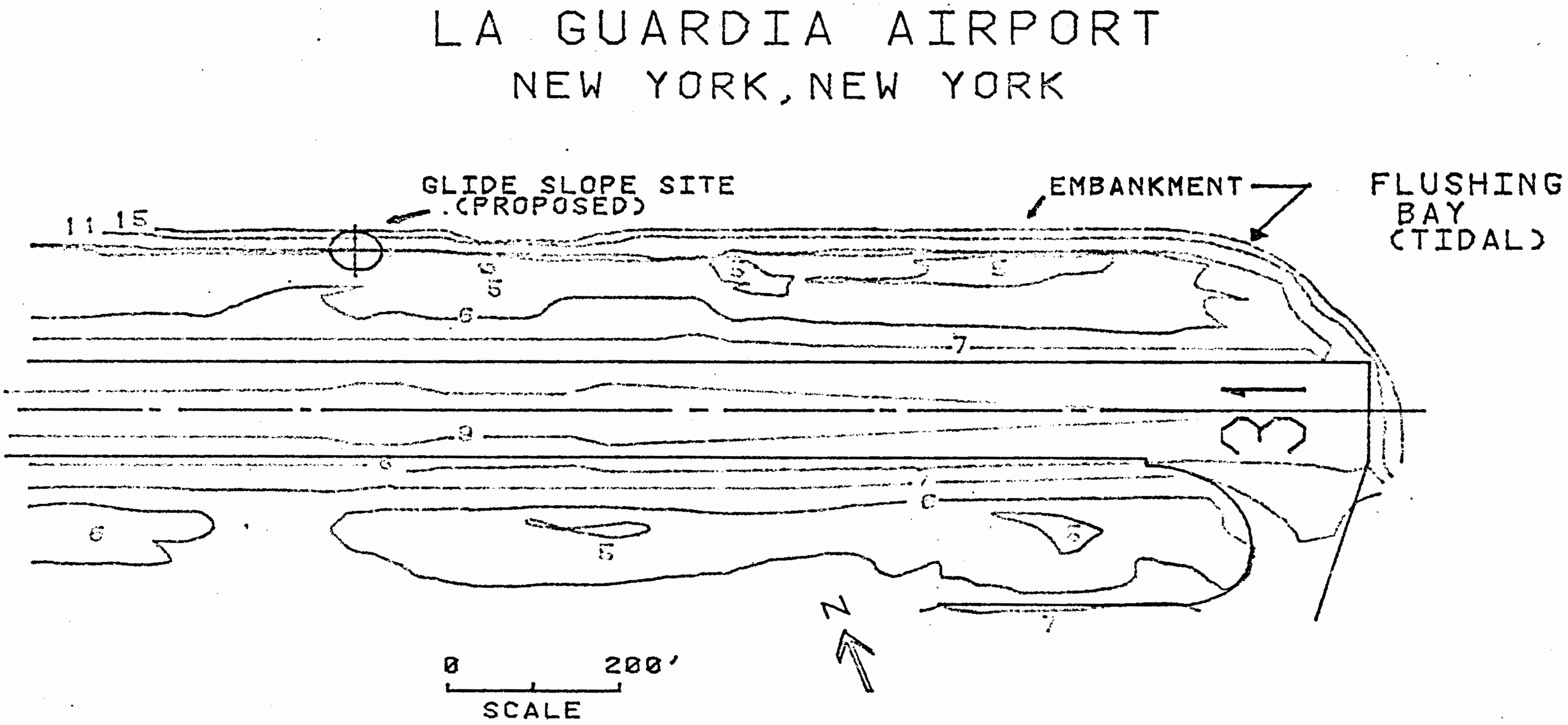

FIGURE 1 - RUNWAY 31, PROPOSED SITE AND TOPOGRAPHY

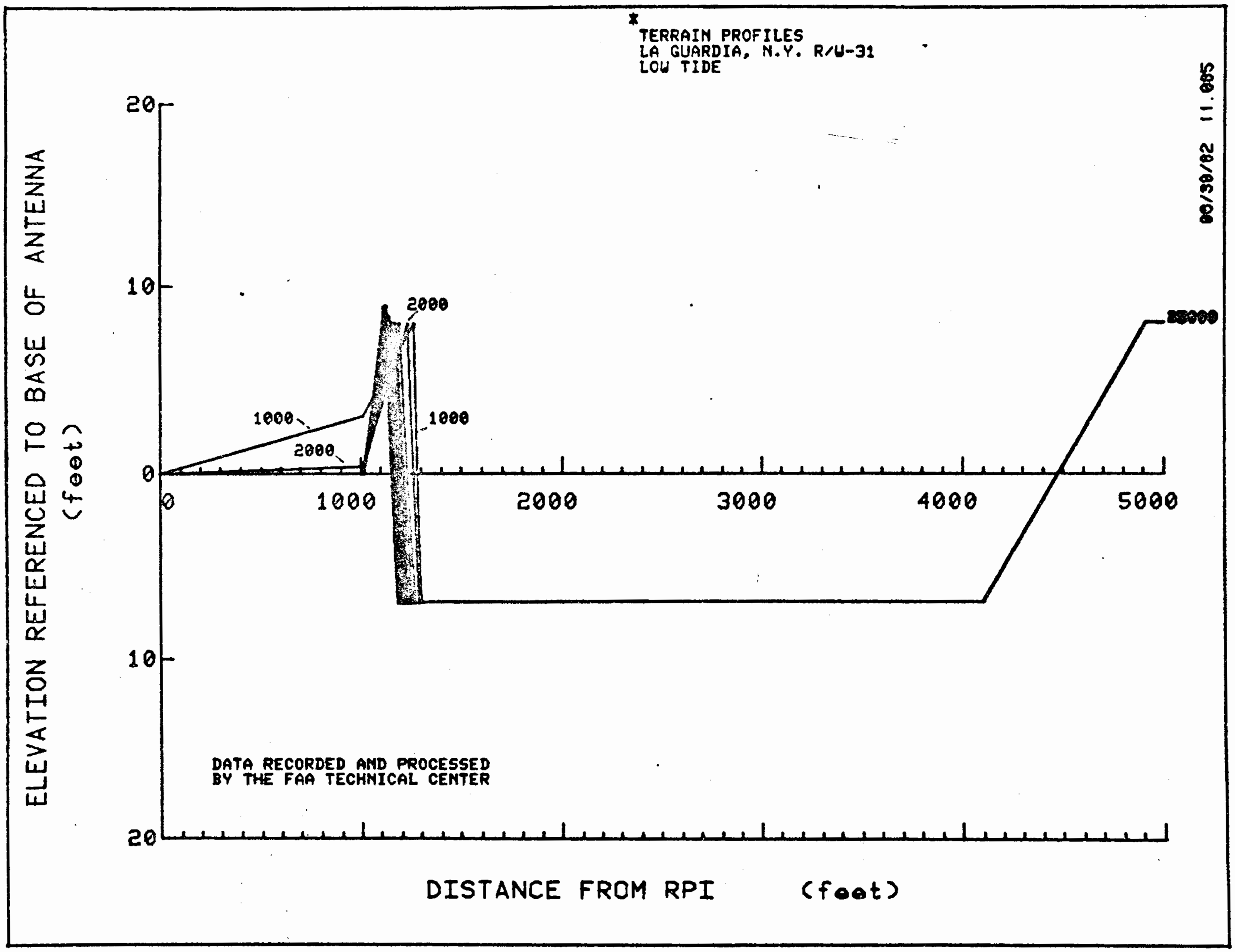

FIGURE 2 - COMPOSITE OF TERRAIN PROFILES, LOW TIDE

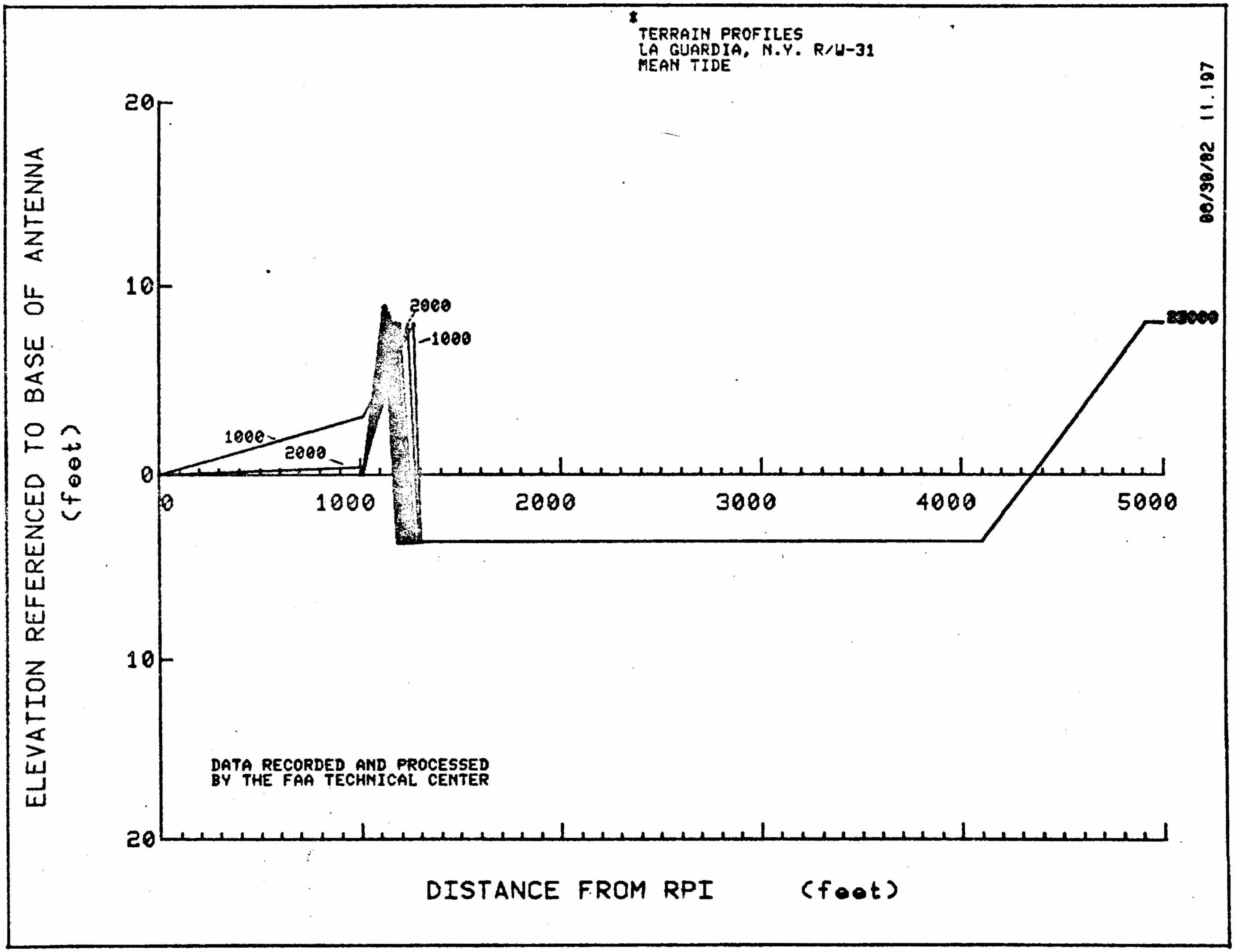

FIGURE 3 - COMPOSITE OF TERRAIN PROFILES, MEAN TIDE

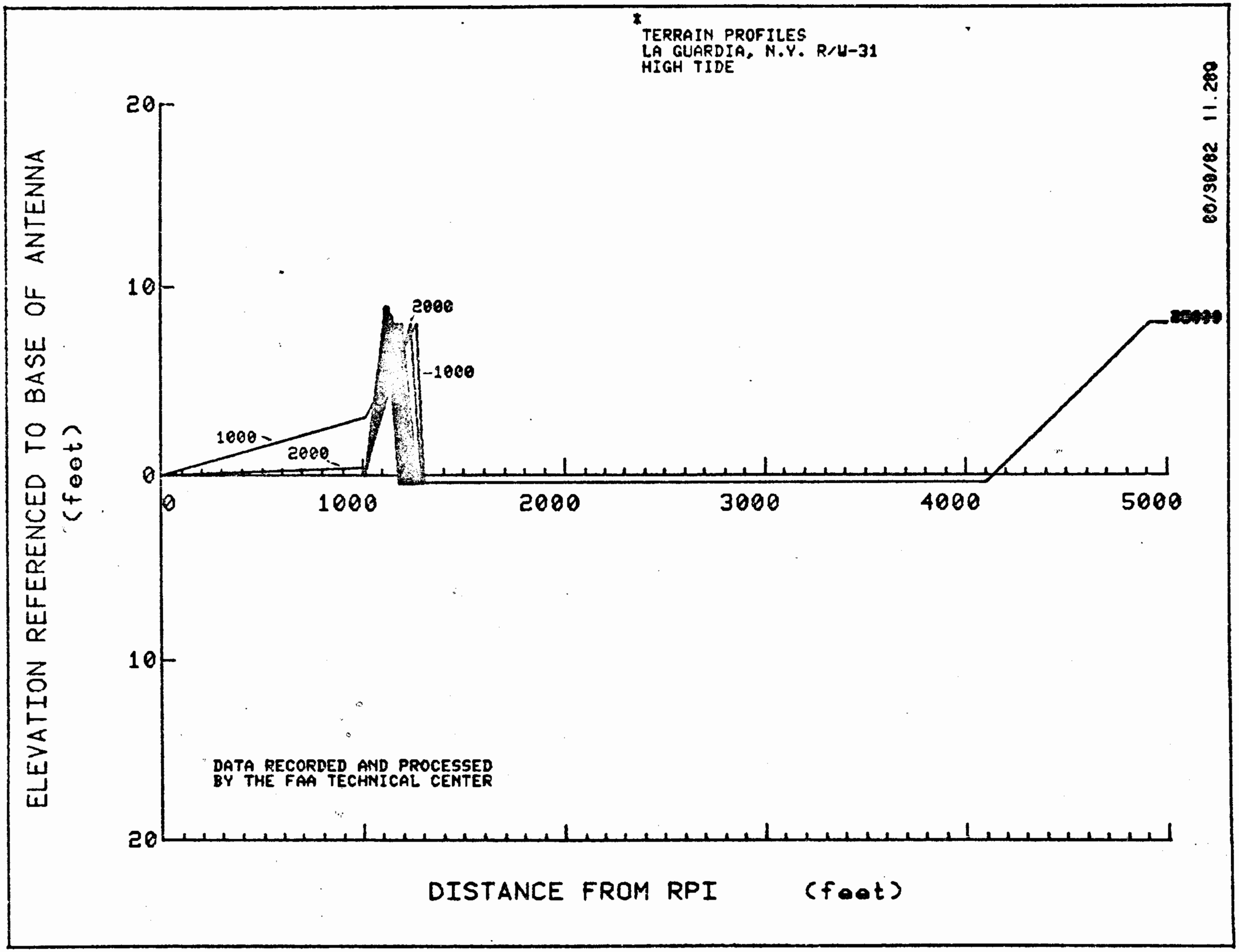

FIGURE 4 - COMPOSITE OF TERRAIN PROFILES, HIGH TIDE

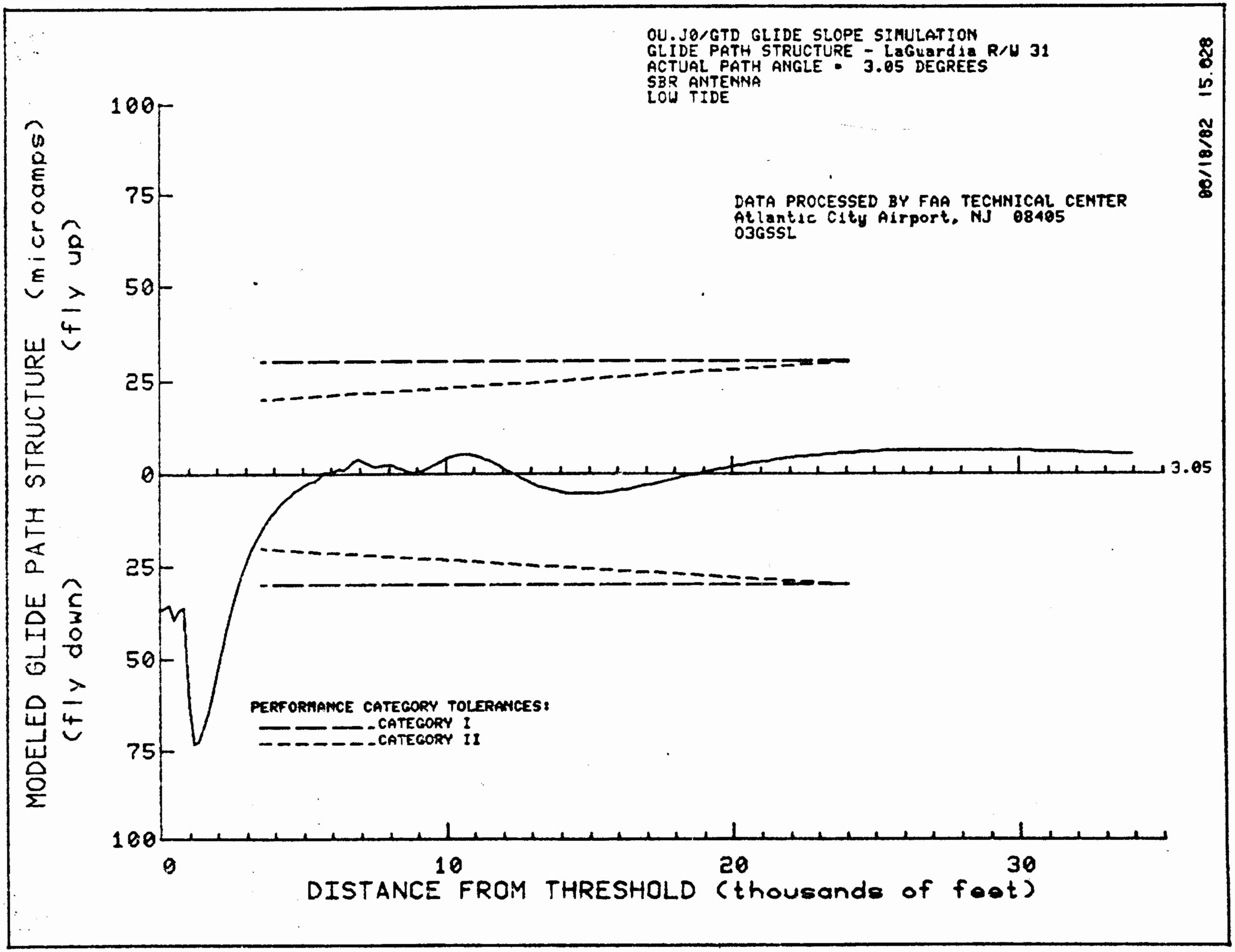

FIGURE 5A - MODELED PATH STRUCTURE, SBR SYSTEM, LOW TIDE

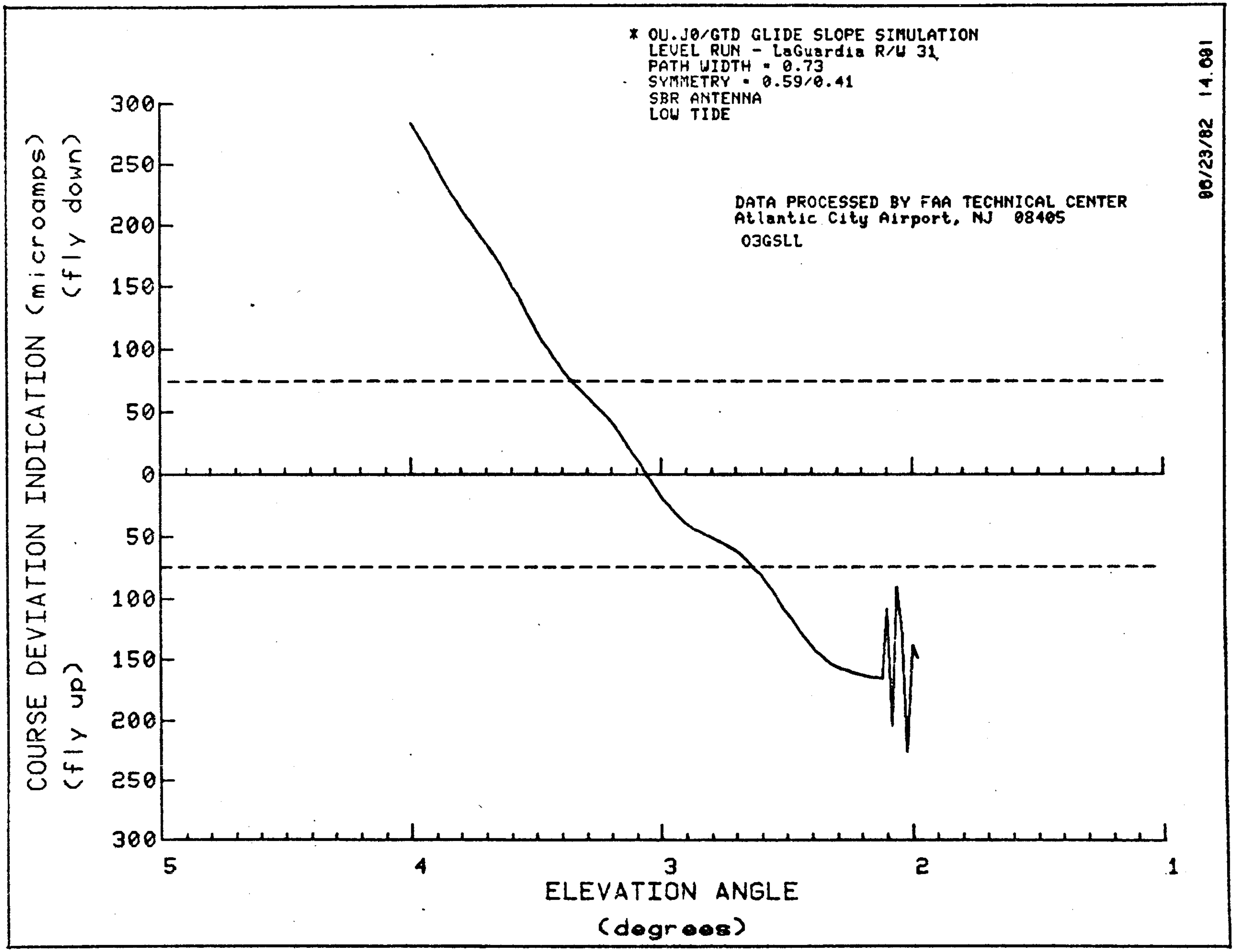

FIGURE 5B - MODELED LEVEL RUN, SBR SYSTEM, LOW TIDE

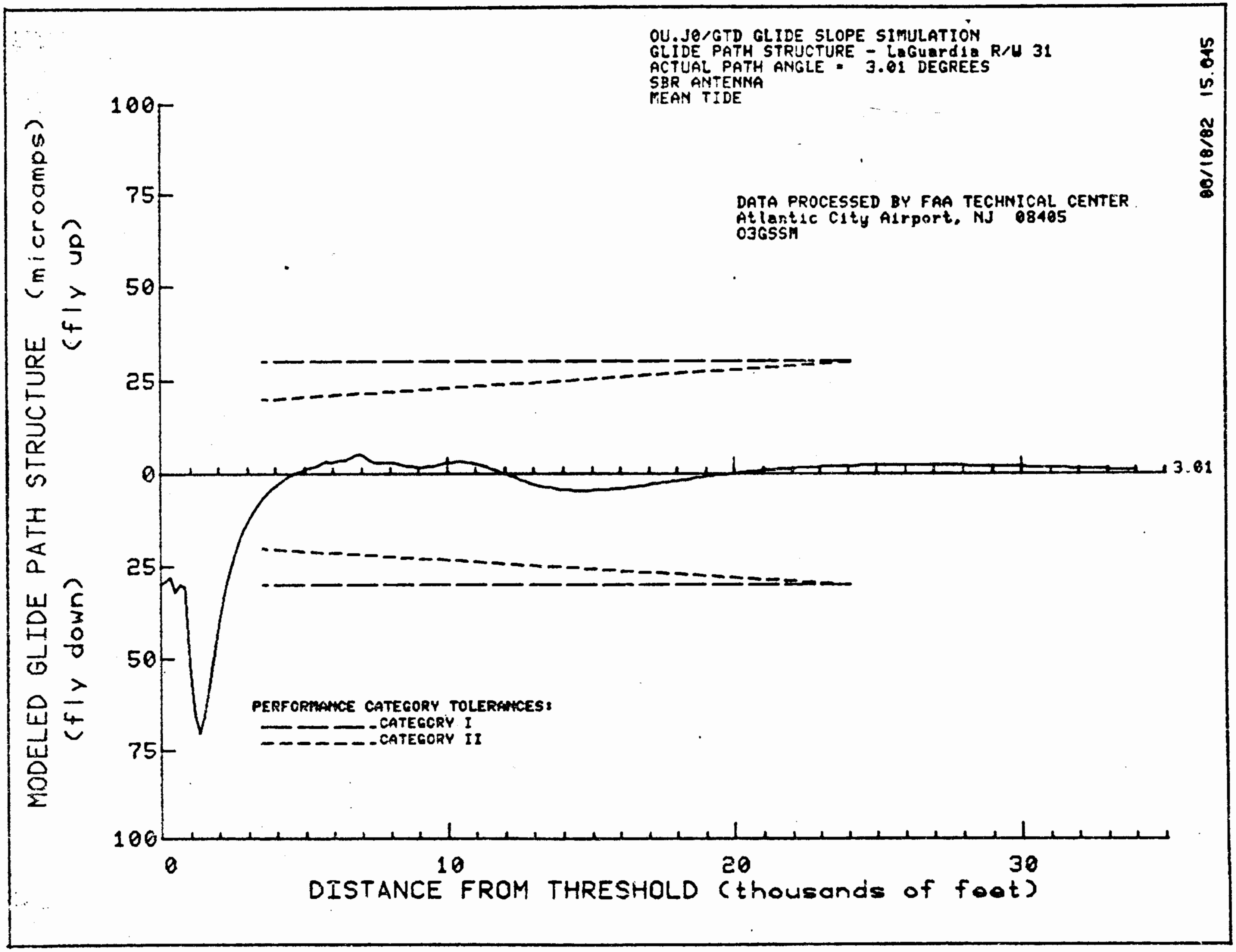

FIGURE 5C - MODELED PATH STRUCTURE, SBR SYSTEM, MEAN TIDE

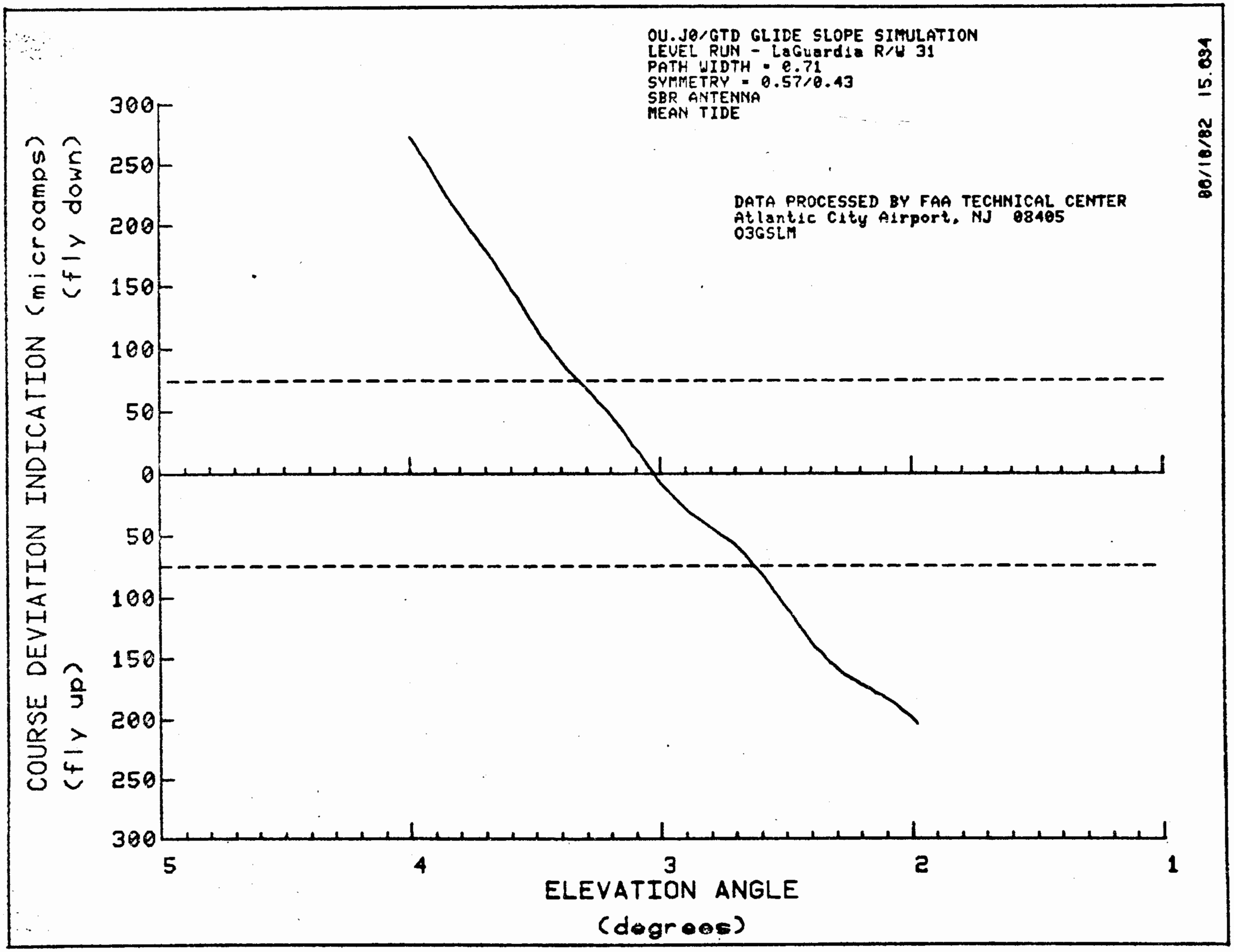

FIGURE 5D - MODELED LEVEL RUN, SBR SYSTEM, MEAN TIDE

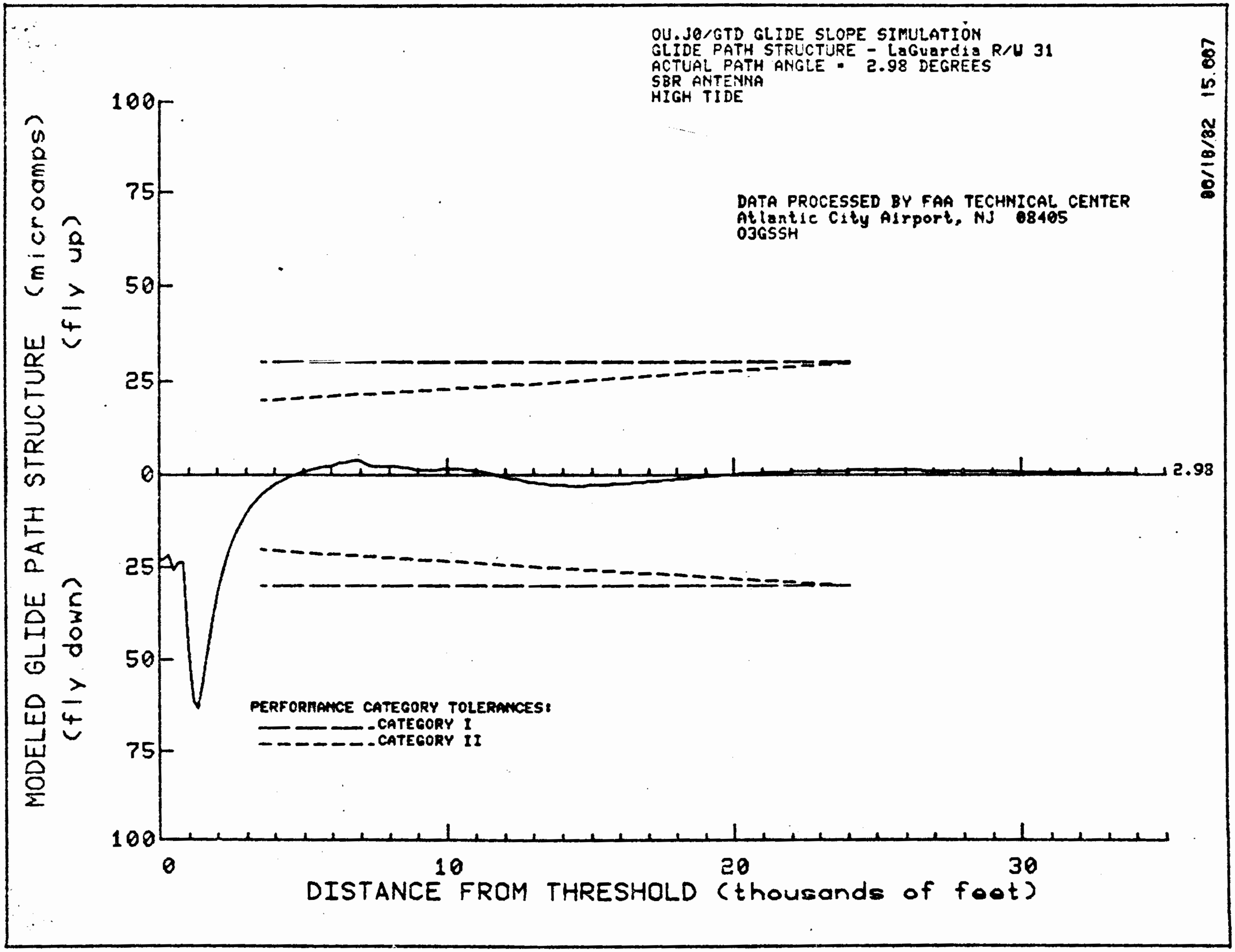

FIGURE 5E - MODELED PATH STRUCTURE, SBR SYSTEM, HIGH TIDE

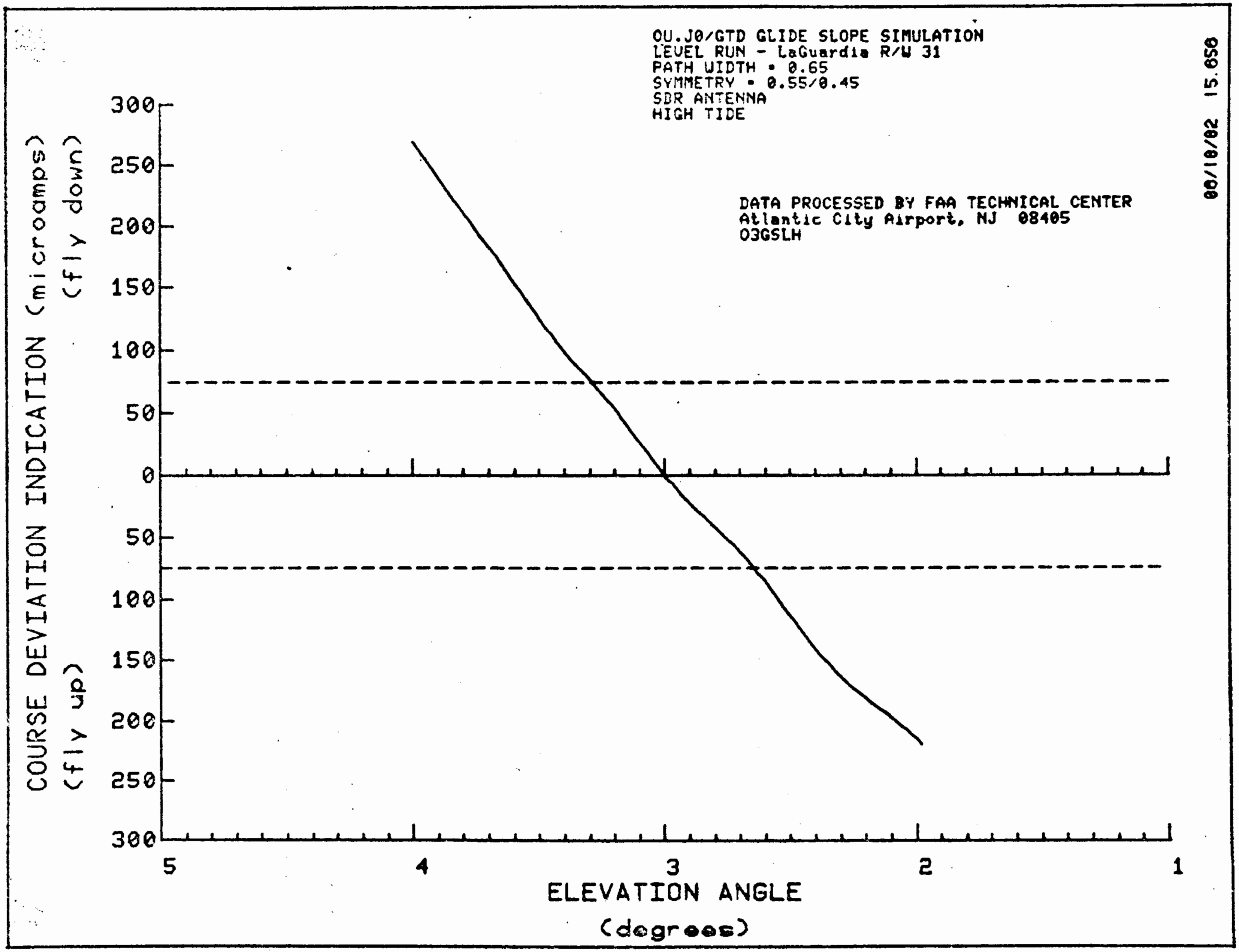

FIGURE 5F - MODELED LEVEL RUN, SBR SYSTEM, HIGH TIDE

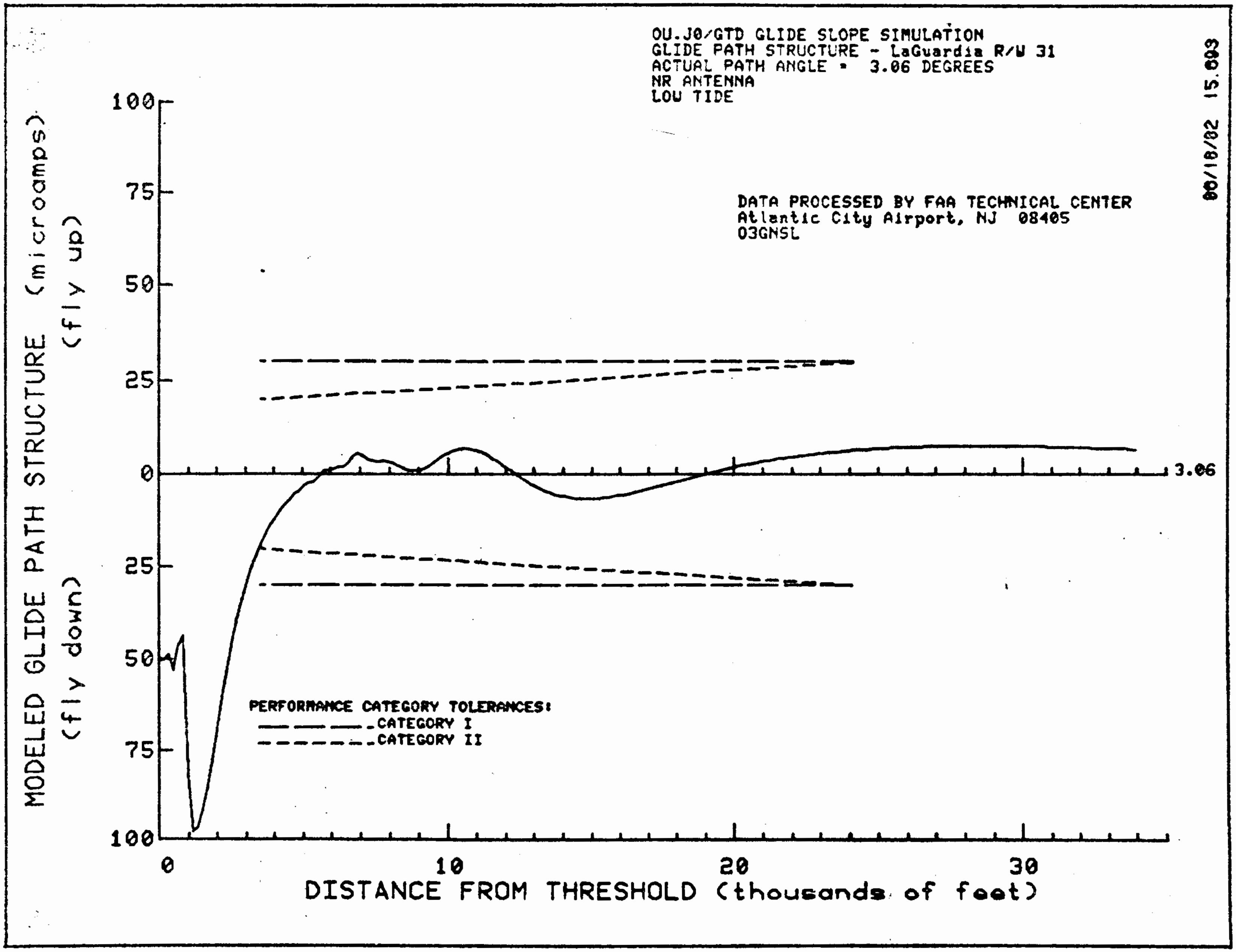

FIGURE 6A - MODELED PATH STRUCTURE, NR SYSTEM, LOW TIDE

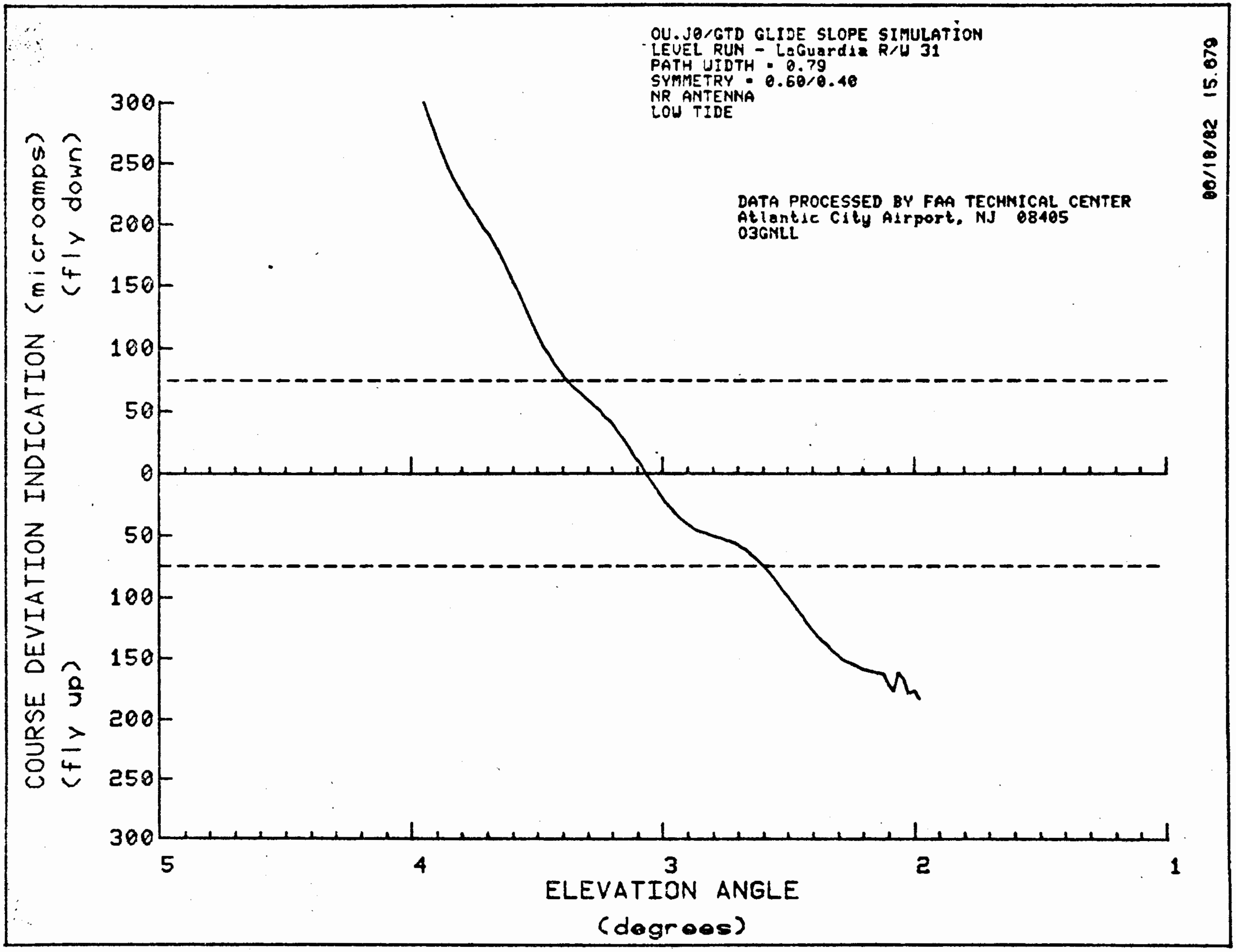

FIGURE 6B - MODELED LEVEL RUN, NR SYSTEM, LOW TIDE

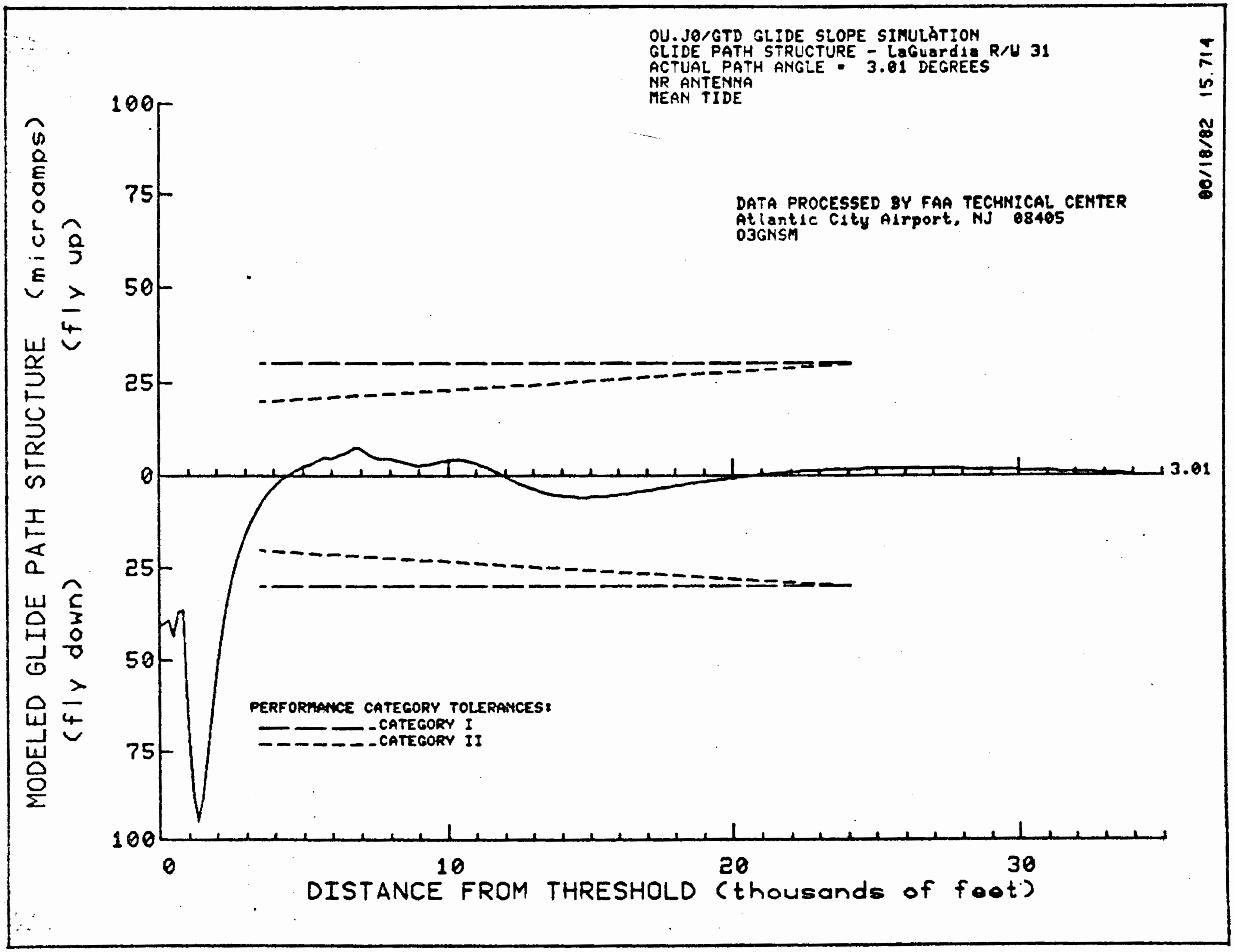

FIGURE 6C - MODELED PATH STRUCTURE, NR SYSTEM, MEAN TIDE

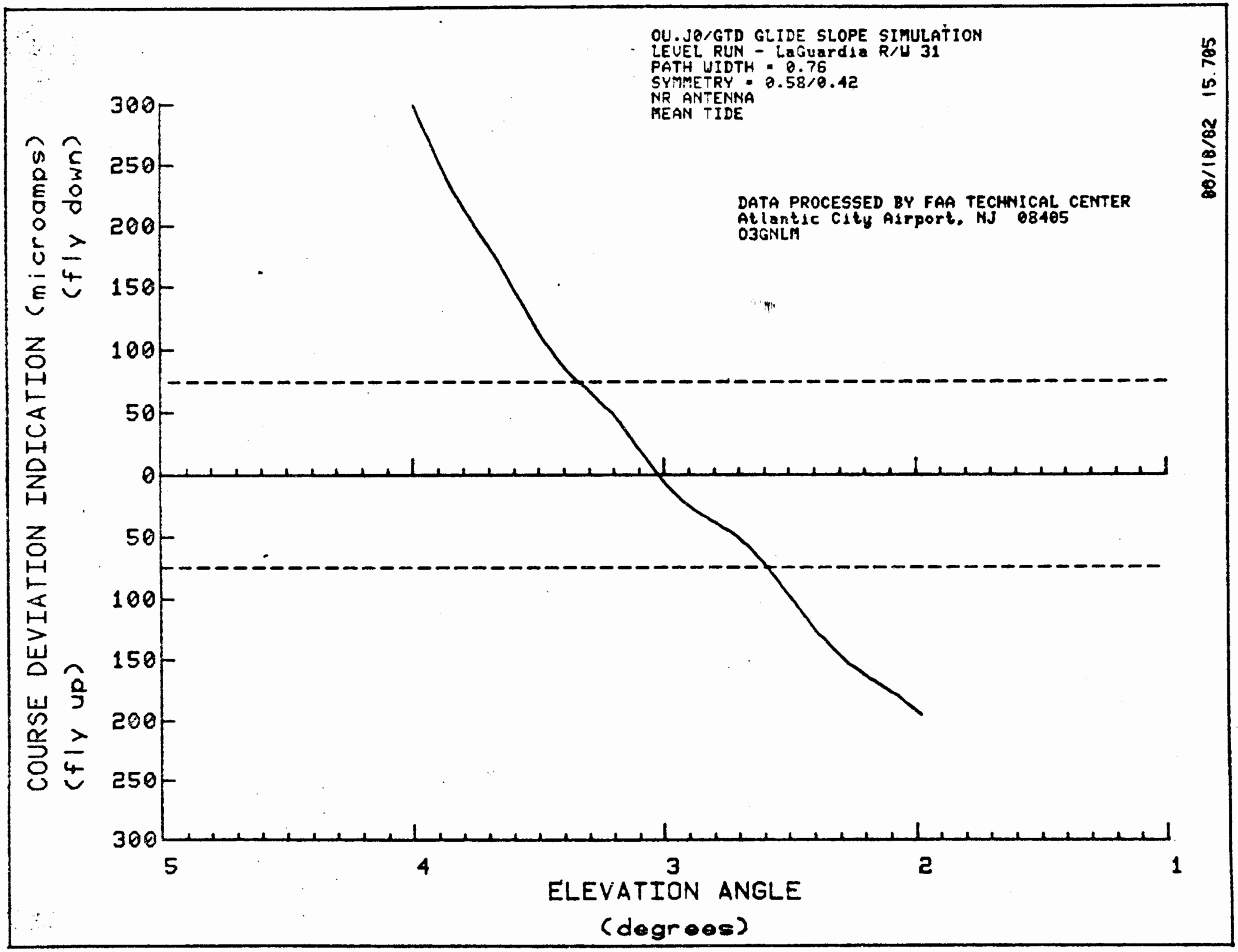

FIGURE 6D - MODELED LEVEL RUN, NR SYSTEM, MEAN TIDE

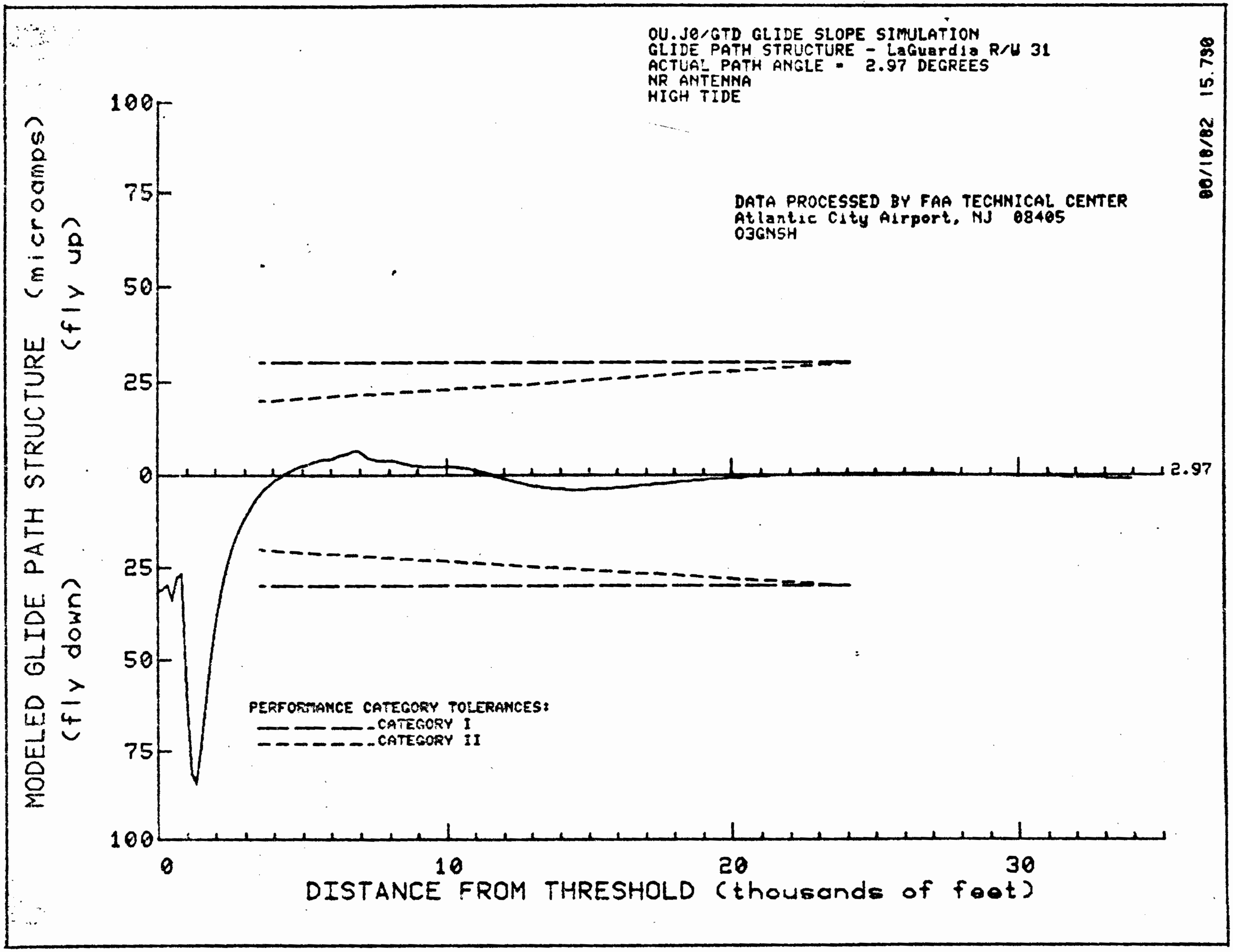

FIGURE 6E - MODELED PATH STRUCTURE, NR SYSTEM, HIGH TIDE

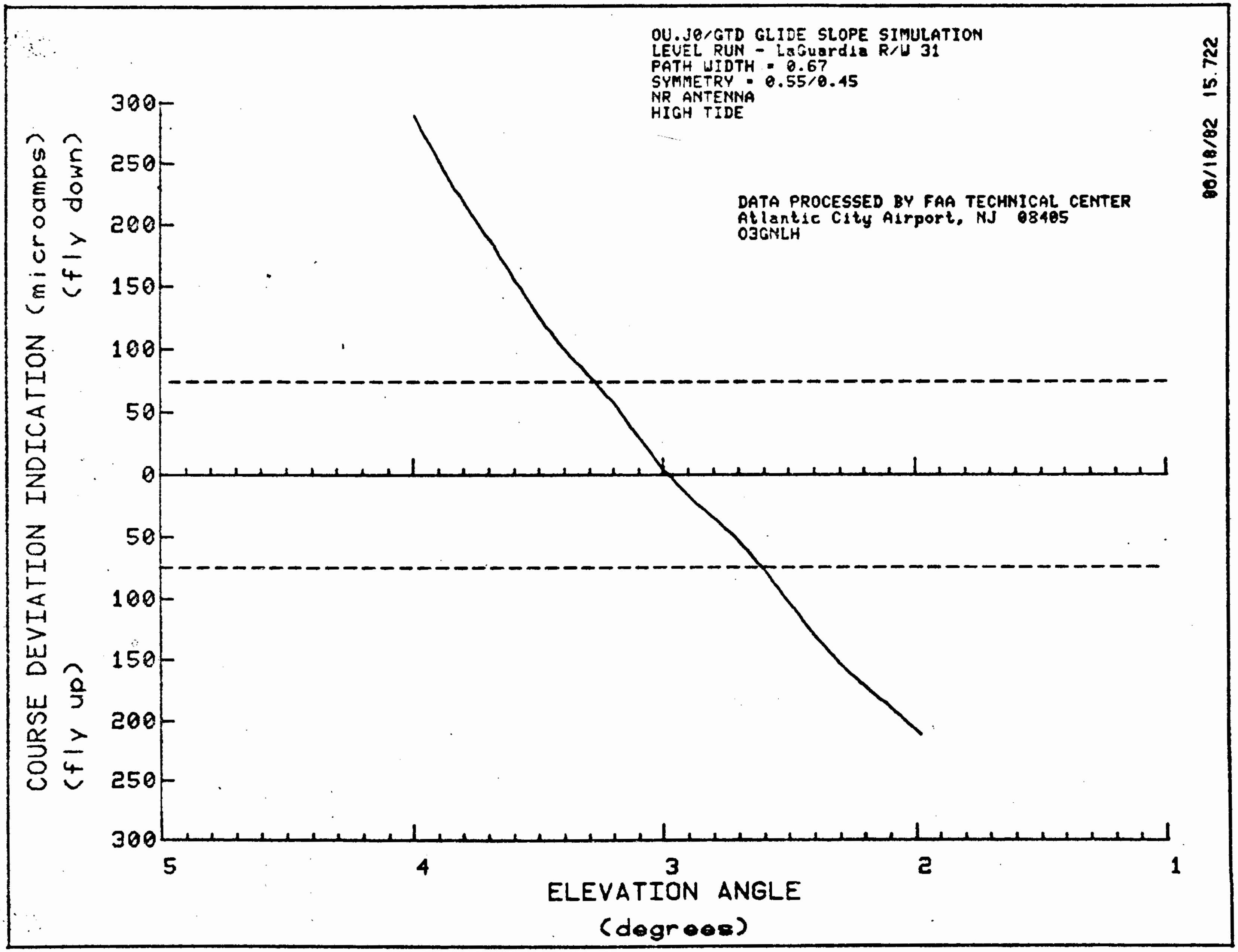

FIGURE 6F - MODELED LEVEL RUN, NR SYSTEM, HIGH TIDE

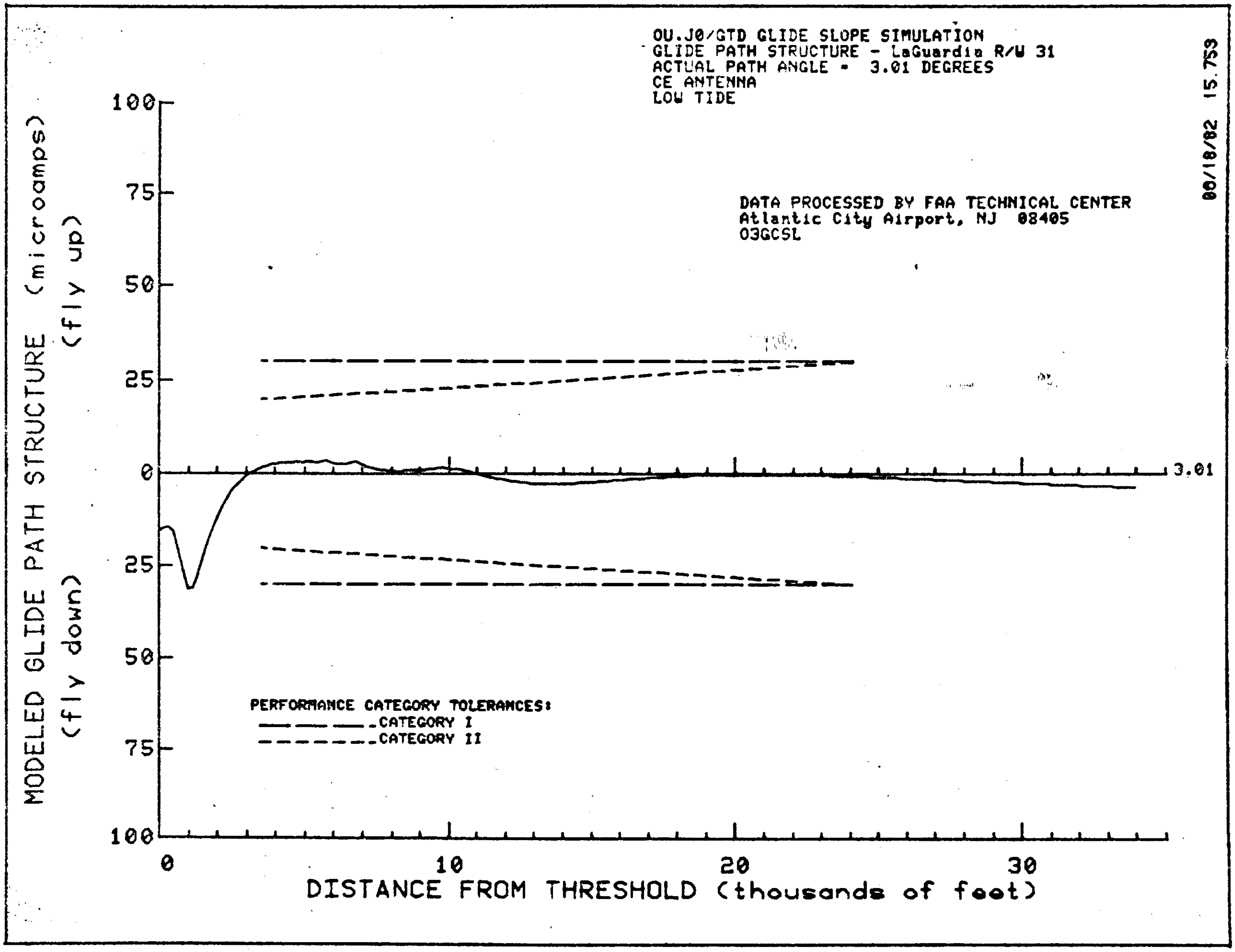

FIGURE 7A - MODELED PATH STRUCTURE, CE SYSTEM, LOW TIDE

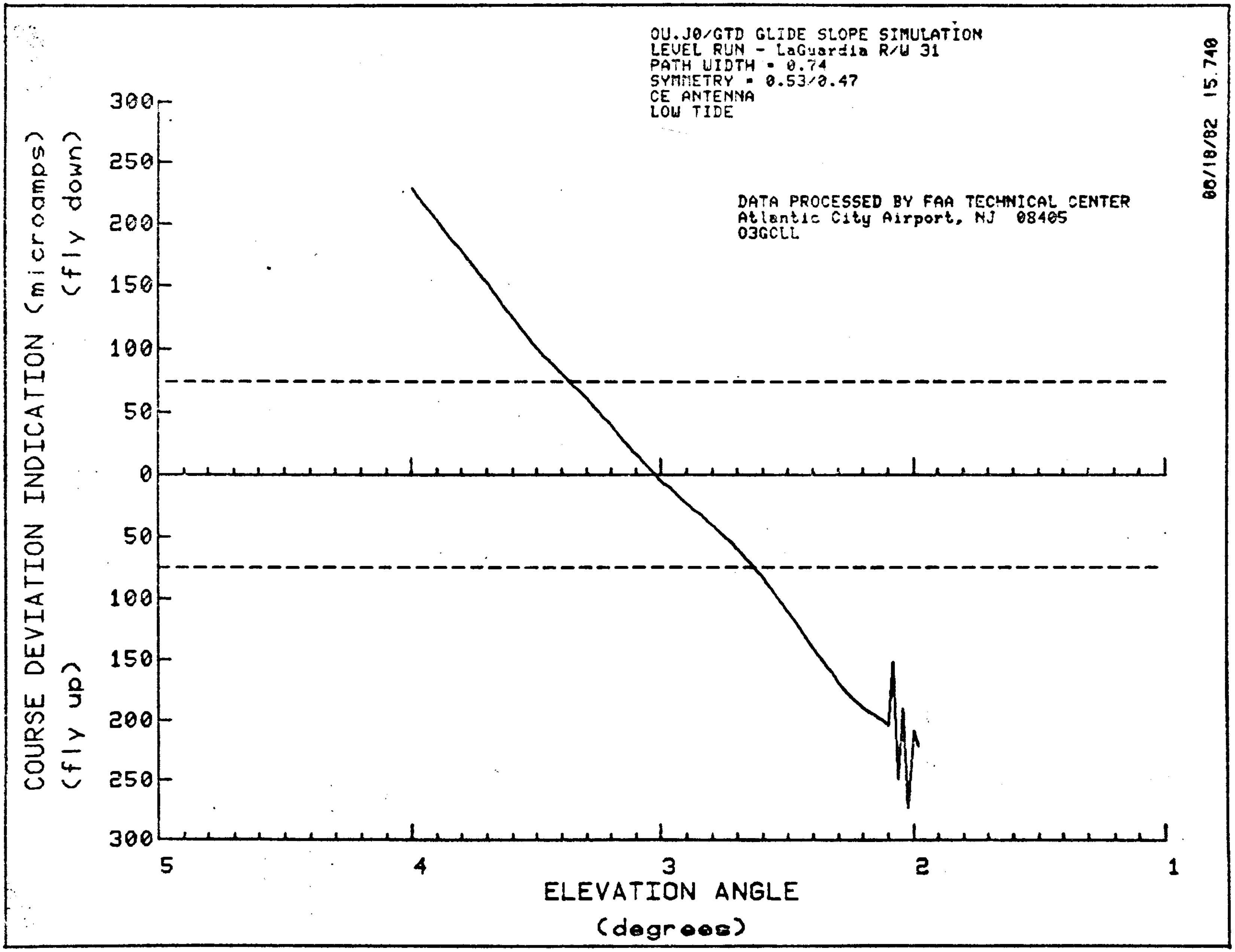

FIGURE 7B - MODELED LEVEL RUN, CE SYSTEM, LOW TIDE

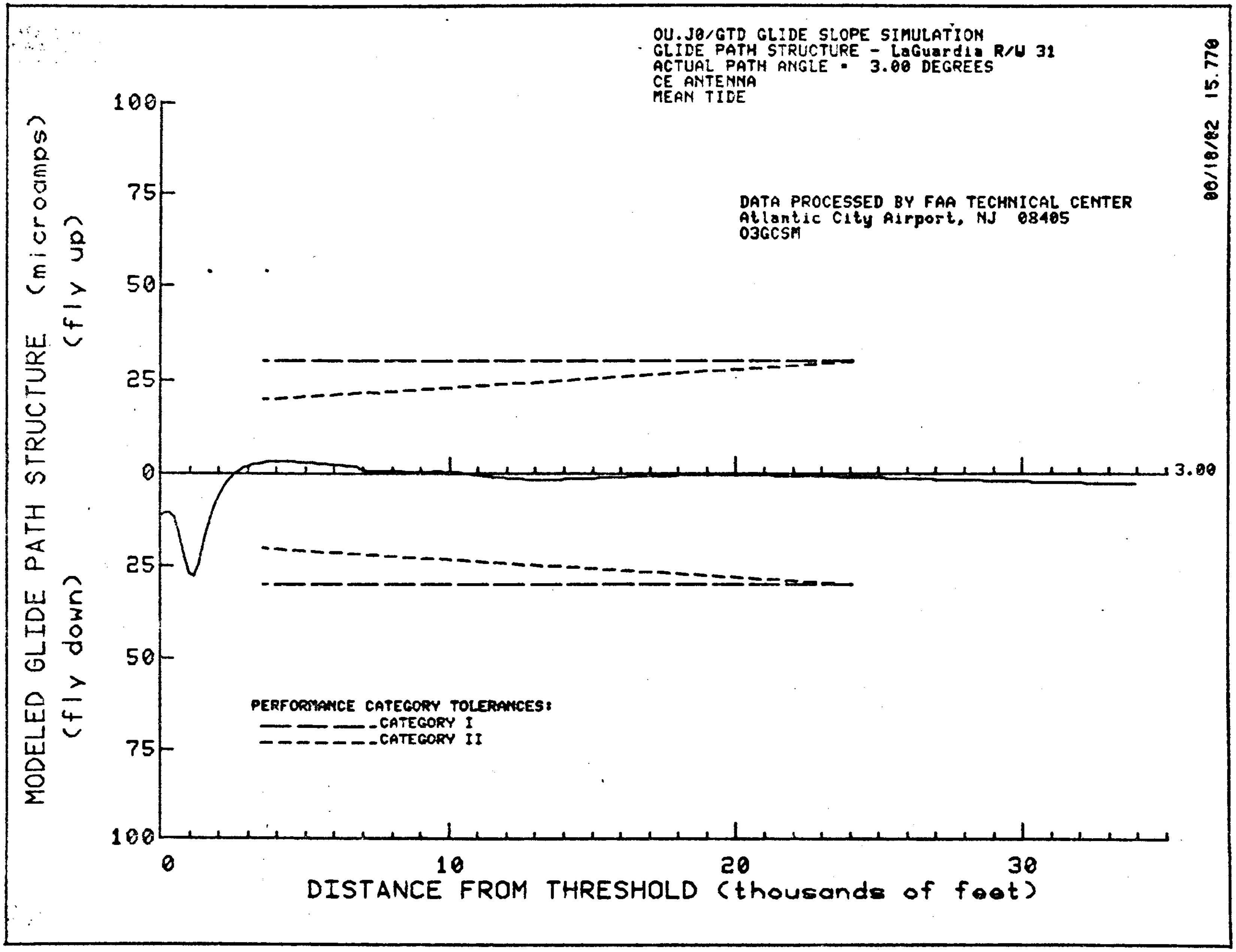

FIGURE 7C - MODELED PATH STRUCTURE, CE SYSTEM, MEAN TIDE

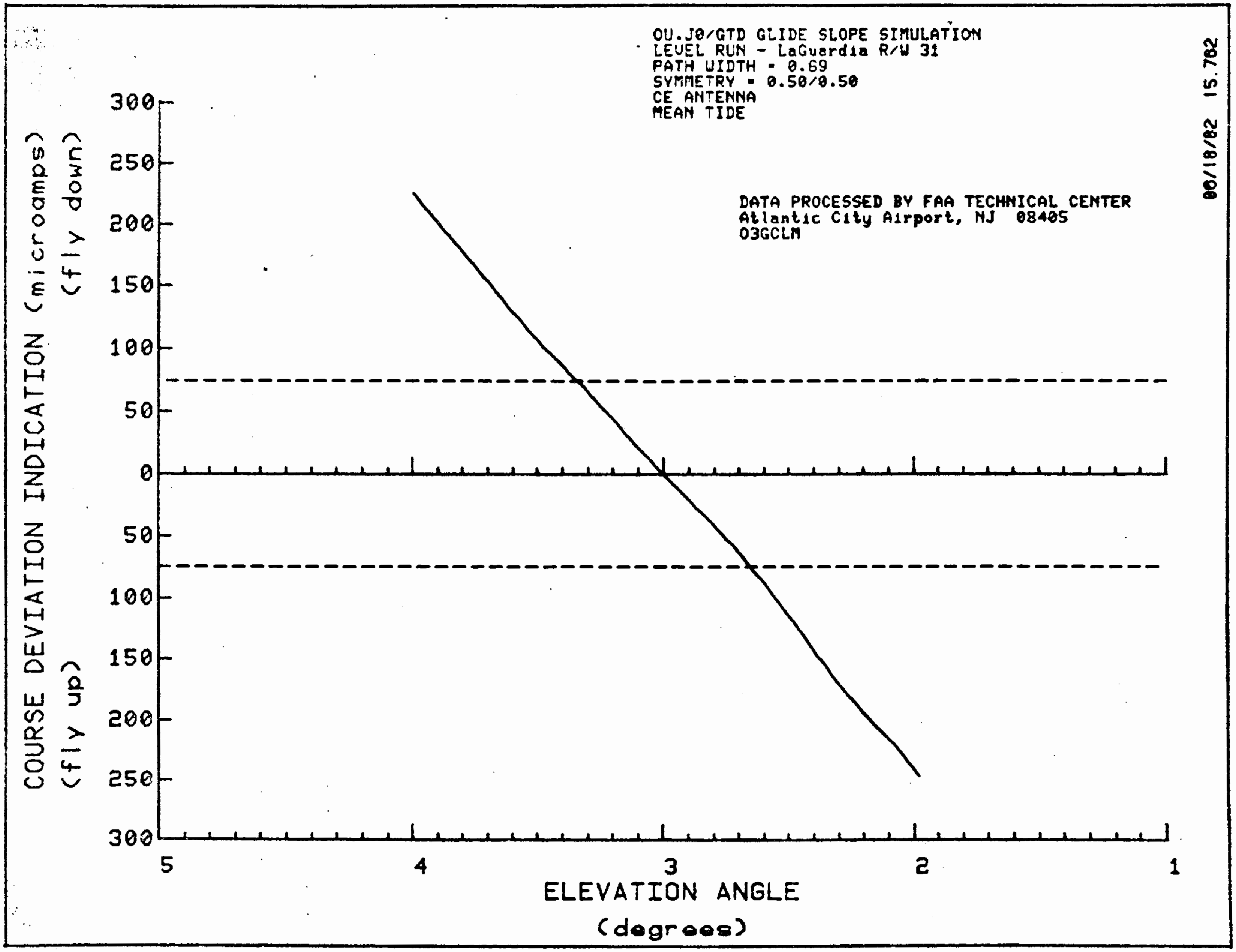

FIGURE 7D - MODELED LEVEL RUN, CE SYSTEM, MEAN TIDE

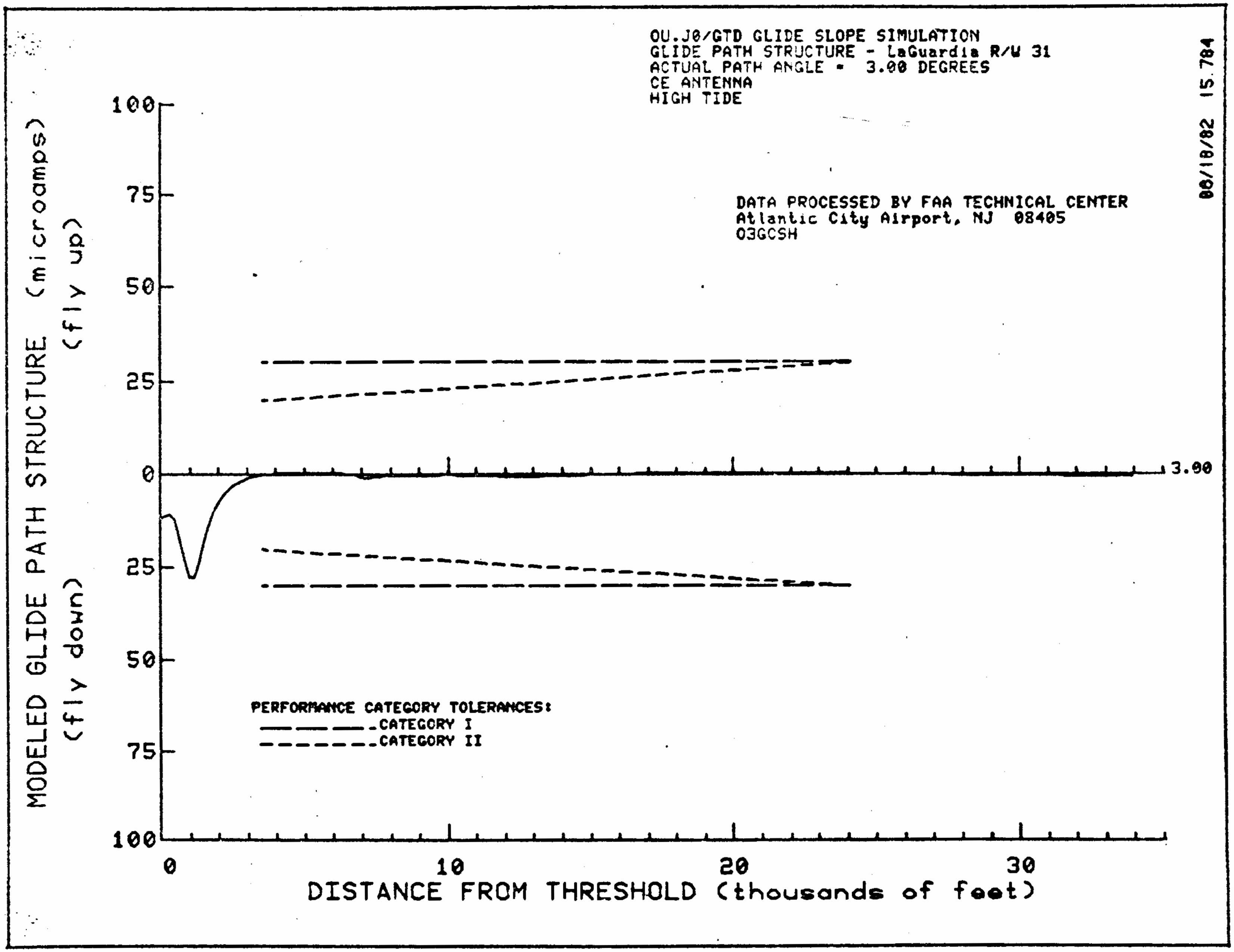

FIGURE 7E - MODELED PATH STRUCTURE, CE SYSTEM, HIGH TIDE

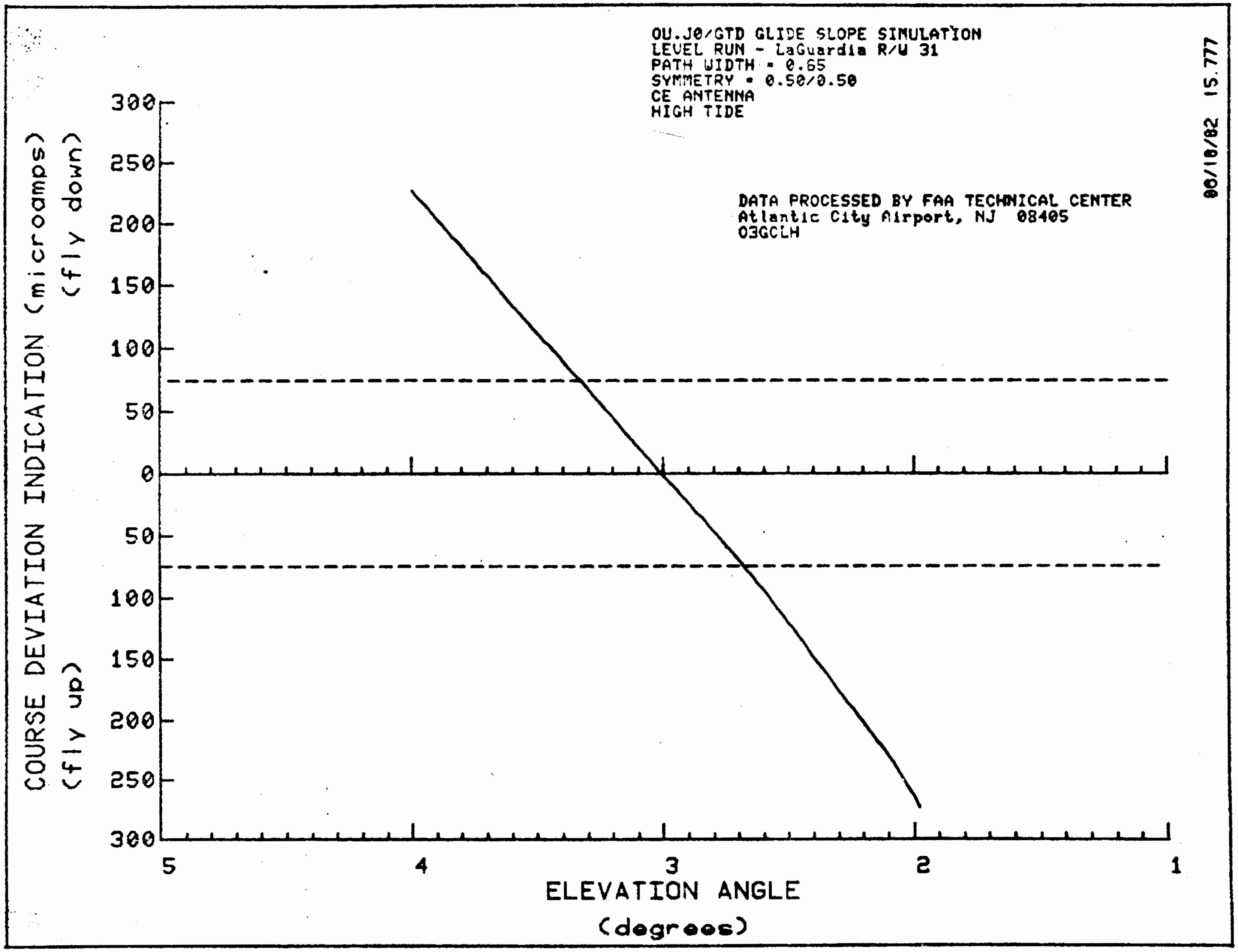

FIGURE 7F - MODELED LEVEL RUN, CE SYSTEM, HIGH TIDE